^{4}He + ^{3}H and ^{4}He + ^{3}He radiative capture, elastic scattering, and electromagnetic properties within the algebraic version of the resonating group model

Alexander S. Solovyev[1,2,*] and Sergey Yu. Igashov[1]

[1]*Dukhov Research Institute of Automatics (VNIIA), 22 Sushchevskaya street, Moscow 127055, Russia*

[2]*Pacific National University, 136 Tikhookeanskaya street, Khabarovsk 680035, Russia*

(Received 15 January 2019; revised manuscript received 27 March 2019; published 17 May 2019)

The mirror seven-nucleon ^{4}He + ^{3}H and ^{4}He + ^{3}He systems are studied microscopically using the algebraic version of the resonating group model. Astrophysical S factors and branching ratios for the ^{3}H$(\alpha,\gamma)^7$Li and ^{3}He$(\alpha,\gamma)^7$Be radiative captures are calculated in a wide energy range from ultralow energies to intermediate ones covering the ^{7}Li and ^{7}Be lowest resonance states. All allowed E1, E2, and M1 captures from s, p, d, and f waves are taken into account in the calculations. Nuclear phase shifts for the ^{3}H$(\alpha,\alpha)^3$H and ^{3}He$(\alpha,\alpha)^3$He s-, p-, d-, and f-wave elastic scattering are computed. Properties of the bound and low-lying resonance states of the ^{7}Li and ^{7}Be nuclei are considered. The obtained results are compared with data from experiments.

DOI: 10.1103/PhysRevC.99.054618

I. INTRODUCTION

At the present time, description of nuclear dynamics and structure from the microscopic viewpoint is a rather significant challenge in modern nuclear theory [1,2]. Microscopic approaches and calculations together with related experimental data serve as an important source of knowledge on nuclear processes. The microscopic calculations, including first principles ones, usually involve some model assumptions and approximations, and questions concerning their accuracy are not clear enough. For this reason, the experimental data are required as essential benchmarks. However, the data are in a number of cases unable to provide the necessary accuracy despite the significant progress in experimental technique. For example, measurements of cross sections of astrophysically relevant nuclear reactions induced by light charged particles at low sub-Coulomb energies meet some difficulties. That is why the relative data are not complete, and their precision turns out to be insufficiently high [3,4]. Thus, the development of the microscopic approaches in fact holds permanent interest to this scientific field [2].

The algebraic version of the resonating group model (AVRGM) [5–7] is a microscopic implementation of the cluster conception in physics of light nuclei and their reactions. A comprehensive description of the AVRGM formalism, namely, the so-called AVRGM basis functions, sets of equations, boundary conditions, and methods for matrix elements calculations, can be found in our work [8] and references cited therein. Within the AVRGM, the total wave function of a system of two clusters is written in the form of a fully antisymmetrized product of the intrinsic wave functions of the clusters and the wave function of their relative motion. The cluster wave functions are usually chosen in the form of the translationally invariant oscillator shell model wave functions for the lowest states compatible with the Pauli exclusion principle. In fact, the conventional RGM [9] and the AVRGM start from this common point. Nevertheless, their further strategies and relative mathematical apparatus significantly differ from each other. The basic idea of the AVRGM is to expand the relative motion wave function over the basis of the oscillator functions. Thus, an expansion of the total wave function over the AVRGM basis functions arises (see Ref. [8] and Appendix A). Values of the oscillator radius for the cluster wave functions and for the oscillator basis are supposed to be the same. An appropriate choice of the oscillator radius playing a role of the scale parameter allows one to improve the approximate description of the internal cluster states. The main idea of the multiscale AVRGM (MS-AVRGM) is to use different values of the oscillator radius involved in expansions of the total wave functions of bound states and continuum. It is quite natural for the wave functions of the different types. The mutual cluster influence can be to some extent taken into account this way. The MS-AVRGM reduces to the simplified case of the single-scale AVRGM (SS-AVRGM) by the unified choice of the oscillator radius in expansions of the total wave functions over the AVRGM basis for all considered states.

In our earlier works [10–17], a microscopic approach based on the SS-AVRGM for radiative capture was developed. Recently, we proposed the more refined MS-AVRGM approach [8,18]. The approaches were implemented to study the mirror radiative capture reactions ^{3}H$(\alpha,\gamma)^7$Li and ^{3}He$(\alpha,\gamma)^7$Be in a low-energy region. These reactions are of significant interest to nuclear astrophysics [3,4,19], and the treatment of them is a striking example of the study, which has a long story and still attracts attention of researchers. A comprehensive list of references to previous experimental and theoretical investigations of these reactions together with a brief discussion can be found in our paper [8]. In recent years, there also appeared a number of other works. First of all, these are experimental measurements of the cross section at low energies for ^{3}H$(\alpha,\gamma)^7$Li in Ref. [20] and for ^{3}He$(\alpha,\gamma)^7$Be

*alexander.solovyev@mail.ru

in Ref. [21] as well as at intermediate energies for the latter reaction in Ref. [22]. A critical review of the ^{3}He$(\alpha,\gamma)^7$Be experimental status has been presented in Ref. [23]. As to the theoretical side, a recent *ab initio* study has been performed in paper [24], where the no-core shell model with continuum (NCSMC) was applied to radiative capture for the first time. Also, the discussed reactions have been considered within potential-model approaches [25,26] and within halo effective field theory [27].

Though many works were devoted to the ^{3}H$(\alpha,\gamma)^7$Li and ^{3}He$(\alpha,\gamma)^7$Be reactions, there is only a small number of studies [22,24,25,28–33], which cover the intermediate energy range including the ^{7}Li and ^{7}Be lowest resonance states. In Refs. [22,33], experimental measurements were carried out for the ^{3}He$(\alpha,\gamma)^7$Be reaction. Experimental data for the mirror one are quite absent at the intermediate energies. Theoretical investigations for the reactions were presented in Refs. [24,25,28–32]. Microscopic calculations were performed solely in Refs. [24,29]. It is obvious here that the microscopic treatment of the considered reactions in the wide energy range is a minor part of the researches in this area. Moreover, this treatment is not free from some difficulties. That is why the further microscopic considerations are still worthwhile.

Thus, the goal of the present work is to study microscopically (i) the ^{3}H$(\alpha,\gamma)^7$Li and ^{3}He$(\alpha,\gamma)^7$Be radiative capture processes in the wide energy range with taking into account all allowed E1, E2, and M1 captures of the colliding nuclei from s, p, d, and f waves of the entrance channel; (ii) the ^{3}H$(\alpha,\alpha)^3$H and ^{3}He$(\alpha,\alpha)^3$He elastic scattering in the s, p, d, and f states; as well as (iii) properties of the bound and low-lying resonance states of the ^{7}Li and ^{7}Be nuclei. The AVRGM serves as the basic tool for this investigation, which significantly extends the scope of our previous work [8]. The performed study allows us to demonstrate descriptive capabilities of our SS- and MS-AVRGM approaches in full.

It should be noted that the mathematical apparatus of expansions over the oscillator basis and the main ingredients of the AVRGM are widely used in modern nuclear physics and give very encouraging results (see, for example, Refs. [1,2,34–38] and references cited therein). This fact produces an additional interest in development of the AVRGM and approaches based on it.

II. ELECTROMAGNETIC MULTIPOLE OPERATORS AND MOMENTS. REDUCED ELECTROMAGNETIC TRANSITION PROBABILITY AND RADIATIVE-CAPTURE PARTIAL CROSS SECTION

The electric multipole operator reads [39,40]

$$M^{\rm E}_{I\mu} = e\sum_{j=1}^{A} g_l(j)|\,\mathbf{r}_j - \mathbf{r}_{\rm c.m.}|^I Y_{I\mu}\left(\mathbf{n}_{\mathbf{r}_j-\mathbf{r}_{\rm c.m.}}\right), \tag{1}$$

$$g_l(j) = \frac{1}{2} - t_{3,j}. \tag{2}$$

Here I is the order of the multipole; $\mathbf{r}_j$ and $t_{3,j}$ are the radius vector and the isospin projection operator of jth nucleon, respectively; A is the mass number of a system; $Y_{I\mu}$ is the spherical harmonic [41]; e is the elementary charge ($e>0$); $\mathbf{r}_{\rm c.m.}$ is the center-of-mass radius vector:

$$\mathbf{r}_{\rm c.m.} = \frac{1}{A}\sum_{j=1}^{A}\mathbf{r}_j. \tag{3}$$

The magnetic multipole operator is defined by [39,40]

$$M^{\rm M}_{I\mu} = \mu_{\rm N}\sum_{j=1}^{A}\left\{g_s(j)\,\mathbf{s}_j + \frac{2g_l(j)}{I+1}\left[(\mathbf{r}_j-\mathbf{r}_{\rm c.m.})\times\left(\mathbf{p}_j - \frac{\mathbf{p}_{\rm c.m.}}{A}\right)\right]\right\}\left(\nabla r^I Y_{I\mu}(\mathbf{n}_{\mathbf{r}})\right)\big|_{\mathbf{r}=\mathbf{r}_j-\mathbf{r}_{\rm c.m.}}, \tag{4}$$

$$g_s(j) = \frac{1}{2}(g_{\rm n}+g_{\rm p}) + t_{3,j}\,(g_{\rm n}-g_{\rm p}),$$
$$g_{\rm n} = -3.826, \qquad g_{\rm p} = 5.586, \tag{5}$$

where $\mu_{\rm N} = e\hbar/2mc$ is the nuclear magneton, $\hbar$ is the Planck constant, c is the light velocity, m is the nucleon mass; $\mathbf{s}_j$ and $\mathbf{p}_j = -\mathrm{i}\nabla_j$ are respectively the spin and momentum operators of jth nucleon; $\mathbf{p}_{\rm c.m.}$ is the center-of-mass momentum operator:

$$\mathbf{p}_{\rm c.m.} = \sum_{j=1}^{A}\mathbf{p}_j. \tag{6}$$

It should be noted that the electric (1) and magnetic (4) multipole operators are written in the long-wavelength limit [39,42]. Moreover, both the operators have the translationally invariant form prescribed by work [43]. This form is required to avoid spurious terms caused by the common center-of-mass motion.

The electric quadrupole and magnetic dipole moments of a nucleus are related to the matrix elements of the corresponding operators (1) and (4) as follows [39]:

$$Q = \sqrt{\frac{16\pi}{5}}\,\langle J^\pi J|M^{\rm E}_{20}|J^\pi J\rangle, \tag{7}$$

$$\mu = \sqrt{\frac{4\pi}{3}}\,\langle J^\pi J|M^{\rm M}_{10}|J^\pi J\rangle, \tag{8}$$

where $|J^\pi J\rangle$ is the nuclear wave function with the total angular momentum J, its projection $M=J$, and the parity π.

TABLE I. The potential parameterizations used in the AVRGM calculations.

Parameterization	$g_{\rm c}$	g_{ls}
I	1.035	1.000
II	1.024	7.869
III	1.024	7.343
IV	0.977	1.000
V	0.977	3.469
VI	0.977	3.025

TABLE II. The oscillator radius values (in fm) involved in the MS-AVRGM bases for the ^{7}Li and ^{7}Be bound states.

Nucleus	Set	$r_{02,0}$	$r_{02,1}$
^{7}Li	I	1.303	1.282
	II	1.296	1.300
^{7}Be	I	1.3068	1.4205
	II	1.3085	1.4240

Since the electromagnetic multipole operator $M^{\Lambda}_{I\mu}$ ($\Lambda \equiv$ E in the electric case or M in the magnetic one) is a tensor operator of rank I with spherical components labeled by μ ($\mu = -I, \ldots, I-1, I$), so its matrix elements satisfy the Wigner–Eckart theorem [41]

$$\left\langle n_f J_f^{\pi_f} M_f \middle| M^{\Lambda}_{I\mu} \middle| n_i J_i^{\pi_i} M_i \right\rangle = \frac{\left\langle n_f J_f^{\pi_f} \middle\| M^{\Lambda}_{I} \middle\| n_i J_i^{\pi_i} \right\rangle}{\sqrt{2J_f+1}} C^{J_f M_f}_{J_i M_i\, I\mu}, \quad (9)$$

in which $\langle n_f J_f^{\pi_f} \| M^{\Lambda}_{I} \| n_i J_i^{\pi_i} \rangle$ is the reduced matrix element; n_i and n_f are additional quantum numbers of the initial (i) and final (f) states, respectively; $C^{J_f M_f}_{J_i M_i\, I\mu}$ is the Clebsch–Gordan coefficient [41]. The reduced transition probability of a nucleus between two bound states with the quantum numbers n_i and $J_i^{\pi_i}$ for the initial state and n_f and $J_f^{\pi_f}$ for the final one can be expressed in terms of the reduced matrix elements of the electromagnetic multipole operator [39]:

$$B\left(\Lambda I, J_i^{\pi_i} \to J_f^{\pi_f}\right) = \frac{1}{2J_i+1} \left| \left\langle n_f J_f^{\pi_f} \middle\| M^{\Lambda}_{I} \middle\| n_i J_i^{\pi_i} \right\rangle \right|^2. \quad (10)$$

The partial cross section for a radiative capture to a final bound state with the total angular momentum J_f and the parity π_f from a partial wave of an initial scattering state normalized to the unit flux density is given by [42]

$$\sigma_{i\to f}(E_{\mathrm{c.m.}}, \Lambda I) = \frac{1}{(2s_1+1)(2s_2+1)(2l_i+1)} \frac{8\pi(I+1)}{\hbar I\left((2I+1)!!\right)^2} \left(\frac{E_\gamma}{\hbar c}\right)^{2I+1} \times \left| \left\langle J_f^{\pi_f} \middle\| M^{\Lambda}_{I} \middle\| J_i^{\pi_i} l_i s_i \right\rangle \right|^2. \quad (11)$$

Here s_1 and s_2 are the spins of the nuclei colliding in the entrance channel of the reaction with the relative motion energy $E_{\mathrm{c.m.}}$ in the center-of-mass system; l_i and s_i are respectively the relative orbital angular momentum and the channel spin that are coupled to the total angular momentum J_i of the initial state with the parity π_i; $E_\gamma = E_{\mathrm{c.m.}} + \varepsilon_n$ is the energy of the emitted photon, ε_n is the breakup threshold for nth bound state of the final fused nucleus into the initial colliding fragments. The colliding nuclei are supposed to be unpolarized, and polarizations of the emitted photon and the formed nucleus are not considered. Therefore, averaging over the spin projections of the projectile and the target and summation over the spin projections of the final products have been performed in Eq. (11). The total cross section can be found by summing up the partial ones (11) characterizing the contributions of the corresponding partial waves in the expansion of the initial scattering wave function. In the long-wavelength limit, the electromagnetic multipole operator entering into Eq. (11) has the form (1) in the electric case or (4) in the magnetic one.

It is generally accepted to write the cross section of a charged-particle induced reaction in terms of the astrophysical S factor [44],

$$\sigma(E_{\mathrm{c.m.}}) = \frac{\exp\left(-\sqrt{E_{\mathrm{G}}/E_{\mathrm{c.m.}}}\right)}{E_{\mathrm{c.m.}}} S(E_{\mathrm{c.m.}}), \quad (12)$$

where E_{G} is the Gamow energy for the colliding particles. Expressing S through σ in accordance with Eq. (12) and substituting Eq. (11) in the obtained expression, one can define the partial astrophysical S factors and, as a result, the total one for a radiative capture.

Let us consider the quantities (7), (8), and (10) for the mirror ^{7}Li and ^{7}Be nuclei within the AVRGM. The expansions in series of the oscillator functions used in the framework of this model (see Appendix A) lead to the corresponding expansion series for the matrix elements of the electromagnetic operators in Eqs. (7), (8), and (10). The electric quadrupole and magnetic dipole moments take the form

$$Q = \sqrt{\frac{16\pi}{5}} \frac{C^{JJ}_{JJ\,20}}{\sqrt{2J+1}} \sum_{\tilde{\nu},\,\nu} C^{(\mathrm{D})}_{J^\pi ls\tilde{\nu}} \left\langle J^\pi ls\tilde{\nu} \middle\| M^{\mathrm{E}}_2 \middle\| J^\pi lsv \right\rangle C^{(\mathrm{D})}_{J^\pi lsv}, \quad (13)$$

$$\mu = \sqrt{\frac{4\pi}{3}} \frac{C^{JJ}_{JJ\,10}}{\sqrt{2J+1}} \sum_{\tilde{\nu},\,\nu} C^{(\mathrm{D})}_{J^\pi ls\tilde{\nu}} \left\langle J^\pi ls\tilde{\nu} \middle\| M^{\mathrm{M}}_1 \middle\| J^\pi lsv \right\rangle C^{(\mathrm{D})}_{J^\pi lsv}, \quad (14)$$

TABLE III. The energies and the widths (in MeV) of the lowest $7/2^-$ and $5/2^-$ resonance states of the ^{7}Li and ^{7}Be nuclei.

Nucleus	J^π	Quantity	Experiment	SS-AVRGM			MS-AVRGM		
				I	II	III	I	II	III
^{7}Li	$7/2^-$	E_{r}	2.18	4.42	2.02	2.18	2.49	2.11	2.18
		Γ	0.069	0.68	0.04	0.05	0.13	0.07	0.08
	$5/2^-$	E_{r}	4.14	4.95	6.38	6.24	2.83	3.28	3.20
		Γ	0.918	1.01	2.55	2.36	0.21	0.36	0.33
^{7}Be	$7/2^-$	E_{r}	2.98	5.36	2.98	3.14	3.35	2.98	3.05
		Γ	0.175	0.89	0.09	0.12	0.22	0.14	0.15
	$5/2^-$	E_{r}	5.14	5.90	7.35	7.21	3.69	4.13	4.06
		Γ	1.2	1.28	3.01	2.80	0.33	0.51	0.48

where the Clebsch–Gordan coefficients have the explicit expressions [41]:

$$C^{JJ}_{JJ\,10} = \sqrt{\frac{J}{J+1}}, \quad C^{JJ}_{JJ\,20} = \sqrt{\frac{J(2J-1)}{(J+1)(2J+3)}},$$

and ν is the number of oscillator quanta. The reduced transition probability is

$$B\left(\Lambda I, J_i^{\pi_i} \to J_f^{\pi_f}\right) = \frac{1}{2J_i+1}\left|\sum_{\nu_f,\,\nu_i} C^{(\mathrm{D})}_{J_f^{\pi_f} l_f s \nu_f} \left\langle J_f^{\pi_f} l_f s \nu_f \middle\| M_I^{\Lambda} \middle\| J_i^{\pi_i} l_i s \nu_i \right\rangle C^{(\mathrm{D})}_{J_i^{\pi_i} l_i s \nu_i}\right|^2. \tag{15}$$

The transition of the ^{7}Li (^{7}Be) nucleus from the first excited state ($J^\pi = 1/2^-$) to the ground one ($J^\pi = 3/2^-$) is accompanied by emission of the photon with the multipolarity $\Lambda I =$ E2 or M1. The total wave functions of these states, which have been considered as the bound ones of the ^{4}He + ^{3}H (^{4}He + ^{3}He) system composed of the unexcited clusters and characterized by $l = 1$ and $s = 1/2$, have been expanded over the AVRGM bases with the coefficients denoted as $C^{(\mathrm{D})}_{J^\pi l s \nu}$.

The partial cross section for the ^{4}He + ^{3}H (^{4}He + ^{3}He) radiative capture with the ^{7}Li (^{7}Be) formation in the framework of the AVRGM has the form

$$\sigma_{i\to f}(E_{\mathrm{c.m.}}, \Lambda I) = \frac{4\pi(I+1)}{(2l_i+1)\hbar I\left((2I+1)!!\right)^2}\left(\frac{E_\gamma}{\hbar c}\right)^{2I+1} \times\left|\sum_{\nu_f,\,\nu_i} C^{(\mathrm{D})}_{J_f^{\pi_f} l_f s \nu_f} \left\langle J_f^{\pi_f} l_f s \nu_f \middle\| M_I^{\Lambda} \middle\| J_i^{\pi_i} l_i s \nu_i \right\rangle C^{(\mathrm{C})}_{J_i^{\pi_i} l_i s \nu_i}\right|^2, \tag{16}$$

in which $C^{(\mathrm{C})}_{J^\pi l s \nu}$ are the expansion coefficients of the total wave function for the ^{4}He + ^{3}H (^{4}He + ^{3}He) scattering state over the AVRGM basis (see Appendix A). In Eq. (16), the quantum numbers (J_i, l_i) are equal to (1/2, 0), (3/2, 2), and (5/2, 2) for the E1 captures, (1/2, 1), (3/2, 1), (5/2, 3), and (7/2, 3) for the E2 ones, as well as (1/2, 1) and (3/2, 1) for the M1 captures to the ground state of the ^{7}Li (^{7}Be) nucleus $[(J_f, l_f) = (3/2, 1)]$. The sum of the corresponding partial cross sections gives the total cross section for the capture to the ground state σ_0. In the case of the ^{7}Li (^{7}Be) first excited state $[(J_f, l_f) = (1/2,\ 1)]$, the list of the allowed quantum numbers are somewhat shorter, namely, (J_i, l_i) are (1/2, 0) and (3/2, 2) for the E1 captures, (3/2, 1) and (5/2, 3) for the E2 ones, and finally (1/2, 1) and (3/2, 1) for the M1 ones. The total cross section for the capture to the first excited state is denoted as σ_1. The sum of σ_0 and σ_1 is the total cross section for the radiative capture, $\sigma = \sigma_0 + \sigma_1$. The corresponding astrophysical S factors are related to these cross sections by Eq. (12). One more quantity used for description of the considered radiative captures is the ratio of the cross sections σ_1 and σ_0, the so-called branching ratio $R = \sigma_1/\sigma_0$.

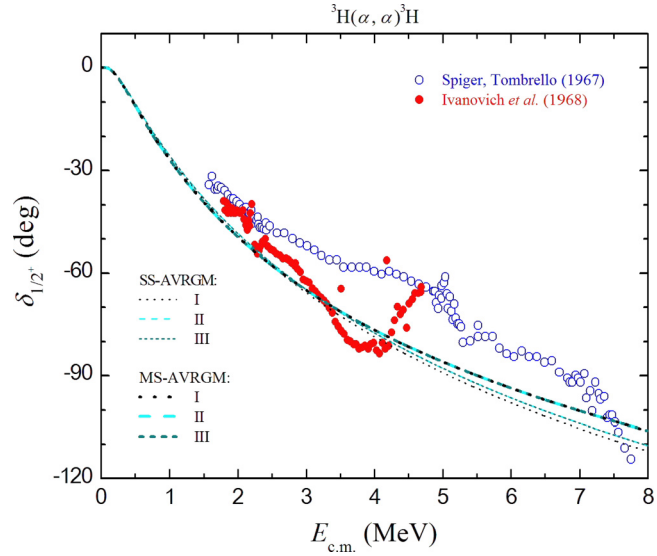

FIG. 1. The $1/2^+$ s-wave nuclear phase shift for the ^{4}He + ^{3}H elastic scattering.

The full set of expressions for all necessary reduced matrix elements involved in Eqs. (13)–(16) is given in Appendix B.

III. RESULTS

A. Introductory remarks and clarifications

In this investigation, the nucleon-nucleon interaction is described by the modified Hasegawa–Nagata NN potential [45] with the intensities of the central Majorana force g_c and the spin-orbit interaction g_{ls}, which are often used as adjustable parameters. Their values adopted in the calculations are given in Table I. Parameterizations I–III and IV–VI from Table I are applied in the SS- and MS-AVRGM calculations, respectively. As it can be seen, parameterizations IV, V, and VI differ

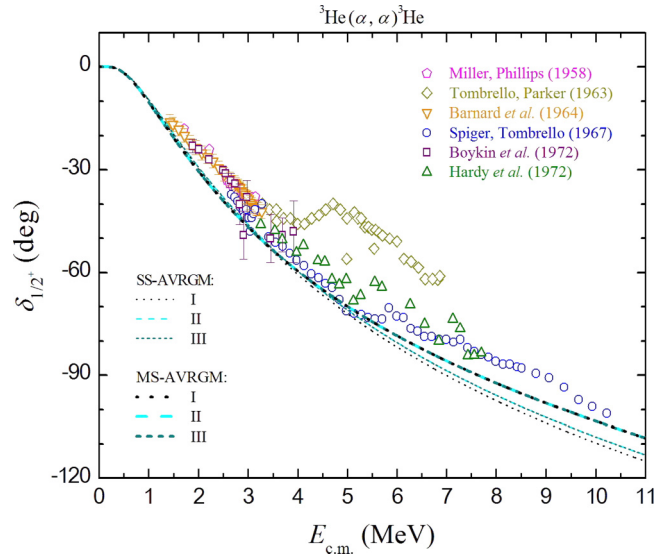

FIG. 2. The $1/2^+$ s-wave nuclear phase shift for the ^{4}He + ^{3}He elastic scattering.

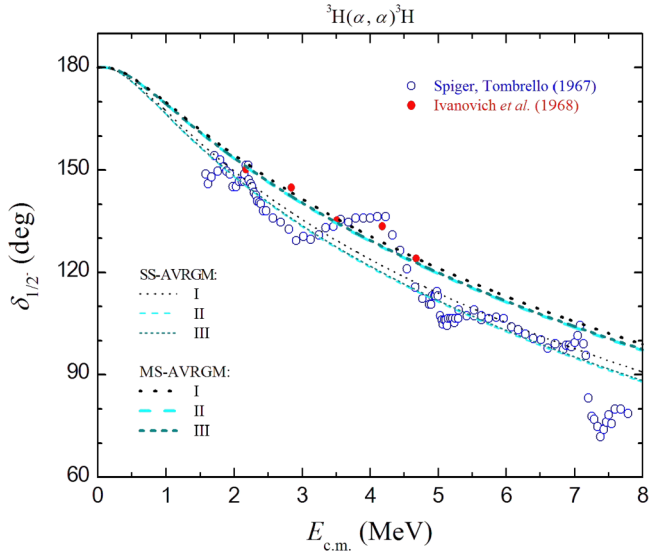

FIG. 3. The $1/2^-$ p-wave nuclear phase shift for the ^{4}He + ^{3}H elastic scattering.

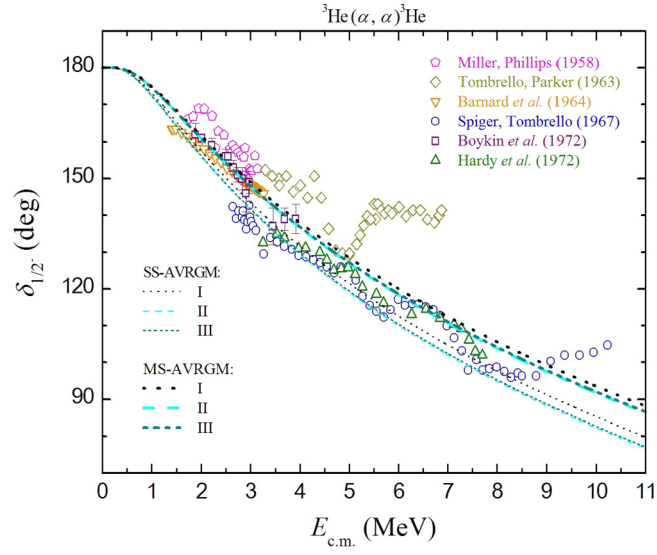

FIG. 5. The $1/2^-$ p-wave nuclear phase shift for the ^{4}He + ^{3}He elastic scattering.

from each other by the g_{ls} values only. This difference for parameterizations V and VI is small enough. The similar situation is in the case of parameterizations II and III. However, parameterization I differs from parameterizations II and III by not only the g_{ls} value but also the g_c one. The reasons for using the different potential parameterizations will be discussed below.

In the framework of the SS-AVRGM approach, the single AVRGM basis with the oscillator radius r_0 is applied for expansions of the total wave functions of all considered states. In the present work, the r_0 value is equal to 1.22 fm. The MS-AVRGM approach deals with the different AVRGM bases for continuous and discrete spectra. These bases differ from each other by values of the oscillator radius. In the continuum, we use $r_{01} = 1.386$ fm for both the ^{4}He + ^{3}H and ^{4}He + ^{3}He systems. Values of the oscillator radius for the ^{7}Li and ^{7}Be ground ($r_{02,0}$) and first excited ($r_{02,1}$) states are presented in Table II. In the following, the calculations using the SS-AVRGM with the given r_0 value and potential parameterizations I–III from Table I will be referred to as SS-AVRGM calculations I–III. The calculation within the MS-AVRGM approach with the chosen r_{01} value and $r_{02,0}$ and $r_{02,1}$ values set I from Table II, as well as with potential parameterization IV from Table I will be referred to as MS-AVRGM calculation I. In turn, the MS-AVRGM calculations combining set II from Table II with potential parameterizations V and VI from Table I will be referred to as MS-AVRGM calculations II and III, respectively.

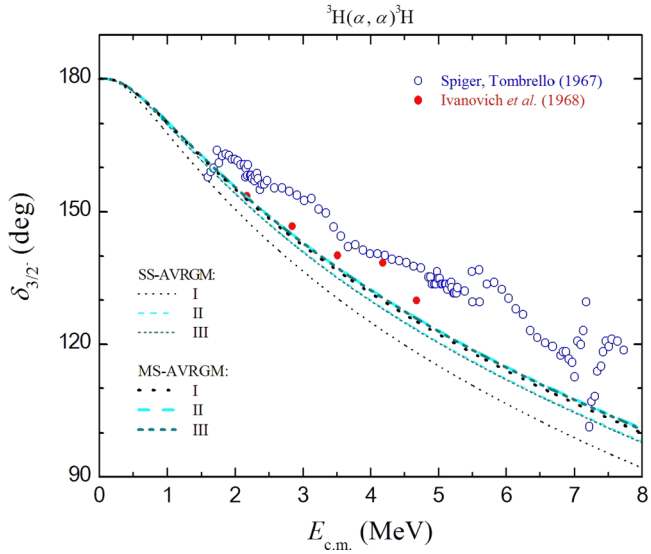

FIG. 4. The $3/2^-$ p-wave nuclear phase shift for the ^{4}He + ^{3}H elastic scattering.

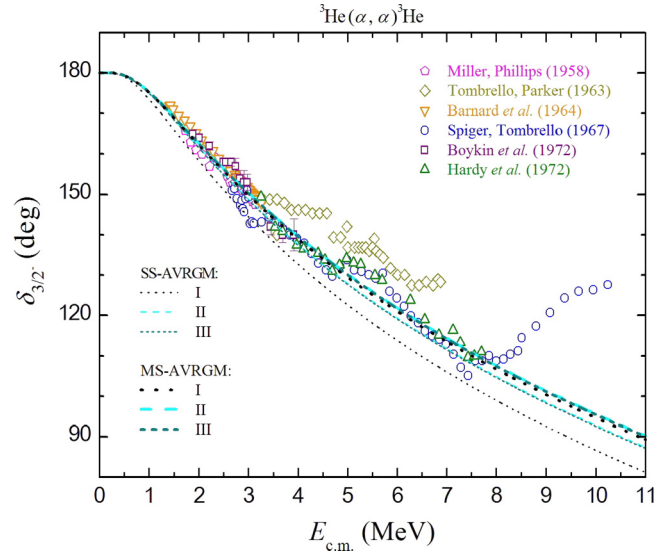

FIG. 6. The $3/2^-$ p-wave nuclear phase shift for the ^{4}He + ^{3}He elastic scattering.

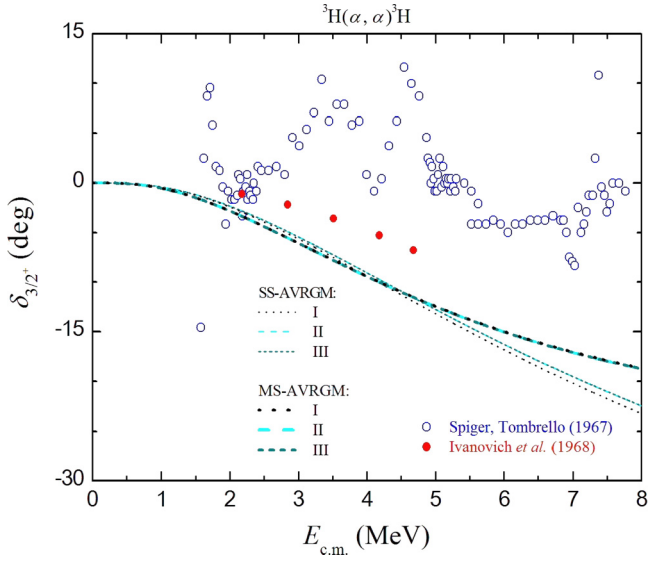

FIG. 7. The $3/2^+$ d-wave nuclear phase shift for the ^{4}He + ^{3}H elastic scattering.

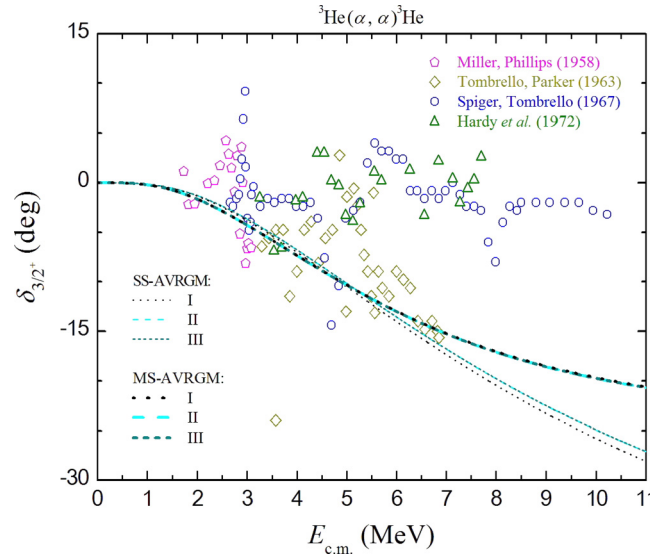

FIG. 9. The $3/2^+$ d-wave nuclear phase shift for the ^{4}He + ^{3}He elastic scattering.

It should be noted that the potential parameterizations and the oscillator radius values utilized in SS- and MS-AVRGM calculations I have been already applied in our previous study [8] for the treatment of the considered systems at astrophysically relevant energies. The adjustable parameters of the potential were fixed in that work to achieve a unified reasonable description of energy dependences for the s- and d-wave nuclear phase shifts of the elastic scattering and for the total astrophysical S factors of the E1 captures in the ^{4}He + ^{3}H and ^{4}He + ^{3}He systems simultaneously. Furthermore, in the case of the MS-AVRGM, the breakup thresholds for the ^{7}Li and ^{7}Be nuclei were reproduced by the appropriate choice of the oscillator radius values. The corresponding calculations of the f-wave nuclear phase shifts performed in the present work show that the positions of the lowest $7/2^-$ and $5/2^-$ resonance states of ^{7}Be and ^{7}Li turn out to be shifted (see Table III, Figs. 11–14, and Sec. III B for details). Parameterizations II and V are introduced for reproducing the position of the lowest $7/2^-$ resonance of ^{7}Be in the SS- and MS-AVRGM approaches, respectively, while parameterizations III and VI are those for ^{7}Li. Moreover, set II of the $r_{02,0}$ and $r_{02,1}$ values is used for improving the MS-AVRGM description of the low-energy experimental data on the total astrophysical S factors related to the captures to the ground and first excited states of the final nucleus.

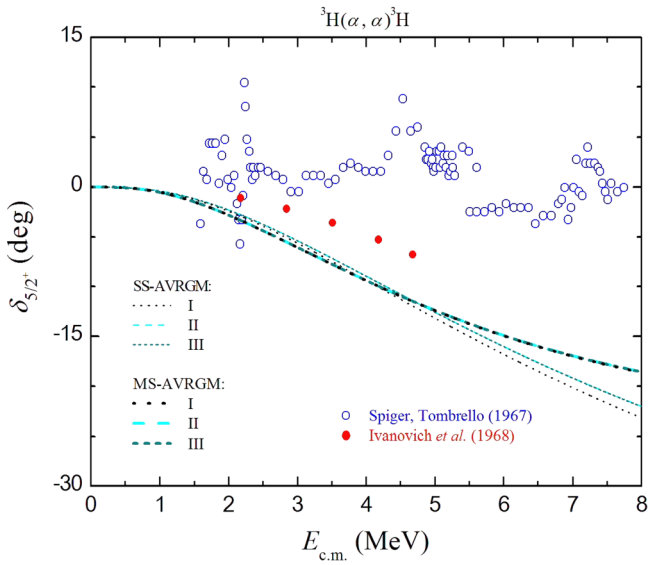

FIG. 8. The $5/2^+$ d-wave nuclear phase shift for the ^{4}He + ^{3}H elastic scattering.

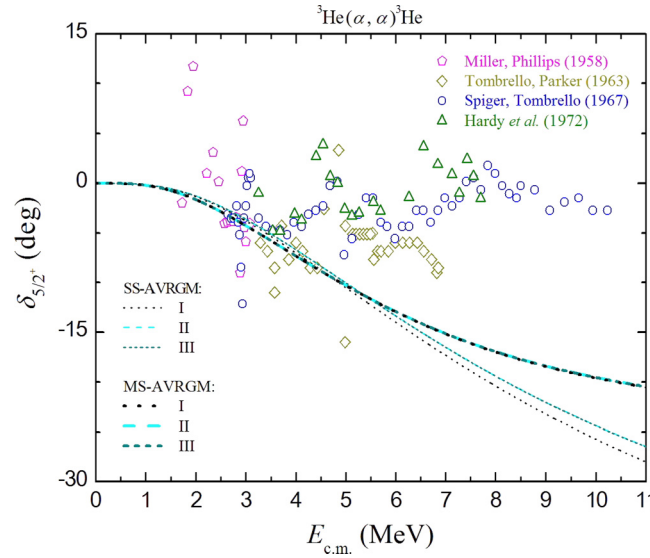

FIG. 10. The $5/2^+$ d-wave nuclear phase shift for the ^{4}He + ^{3}He elastic scattering.

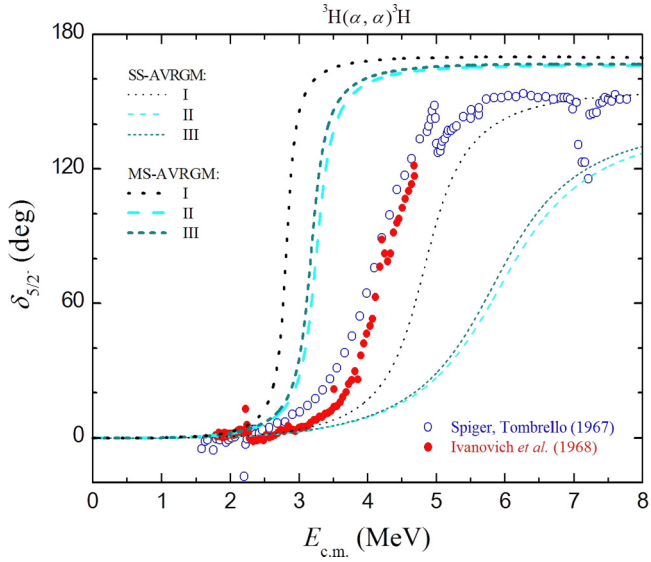

FIG. 11. The $5/2^-$ f-wave nuclear phase shift for the ^{4}He + ^{3}H elastic scattering.

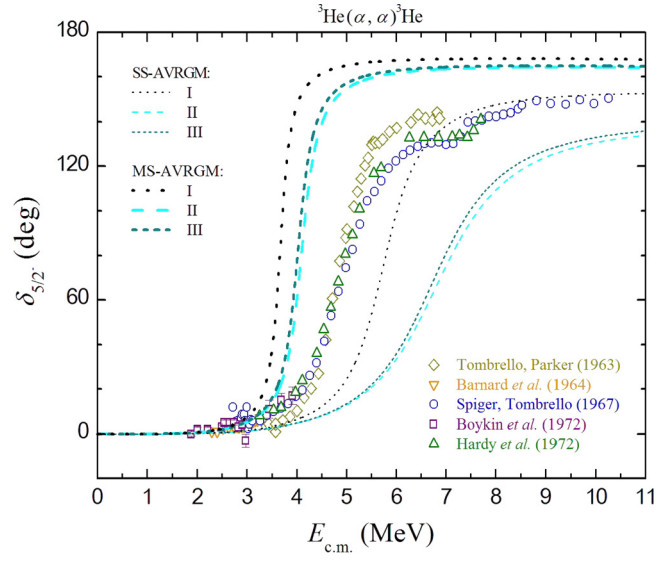

FIG. 13. The $5/2^-$ f-wave nuclear phase shift for the ^{4}He + ^{3}He elastic scattering.

B. The ^{3}H(α, α)^{3}H and ^{3}He(α, α)^{3}He elastic scattering

Energy dependences of the nuclear phase shifts for the ^{4}He + ^{3}H and ^{4}He + ^{3}He elastic scattering calculated within the SS- and MS-AVRGM approaches are depicted in Figs. 1–14 together with data extracted from experiments [46–52]. The calculated phase shifts correspond to all partial waves with the orbital angular momentum $l = 0$, 1, 2, and 3 that are required for description of the E1, E2, and M1 radiative-capture processes in the discussed systems at the considered energies. Before we begin the discussion of the phase shifts, it should be emphasized that the data for ^{4}He + ^{3}H and most data for ^{4}He + ^{3}He obtained from the elastic scattering measurements were published without experimental errors. This feature essentially complicates a question concerning a degree of agreement between the AVRGM calculations and the data. Nevertheless, some conclusions on this agreement will be given in this subsection.

All the AVRGM calculations of the s-wave nuclear phase shift presented in Fig. 1 for the ^{4}He + ^{3}H scattering agree reasonably with the data [50]. The data [49] are mainly located higher than those of Ref. [50] and our curves. In the case of the mirror system, the corresponding calculations of the s-wave phase shift are on the whole in a good agreement with all the data, excepting the data [47] that lie higher than the others (see Fig. 2). The p-wave nuclear phase shifts are demonstrated for ^{4}He + ^{3}H in Figs. 3 and 4 and for ^{4}He + ^{3}He in Figs. 5 and 6. In the case of the ^{4}He + ^{3}H scattering, the

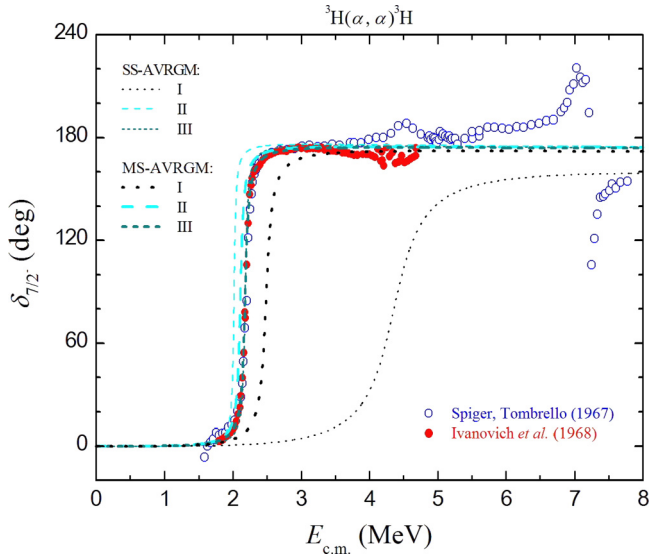

FIG. 12. The $7/2^-$ f-wave nuclear phase shift for the ^{4}He + ^{3}H elastic scattering.

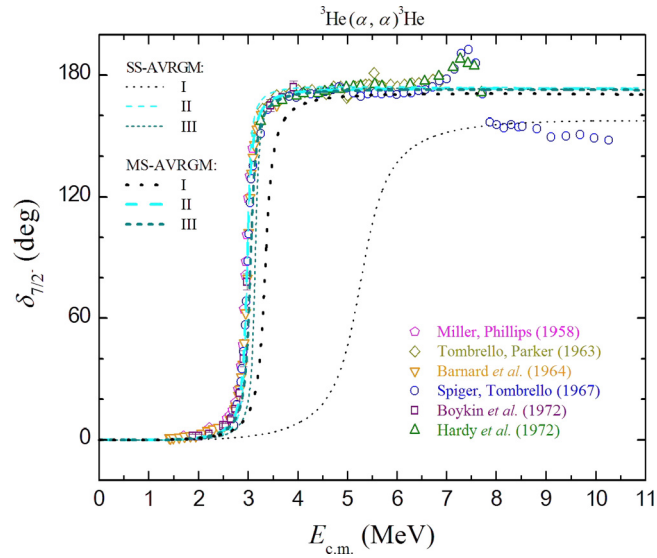

FIG. 14. The $7/2^-$ f-wave nuclear phase shift for the ^{4}He + ^{3}He elastic scattering.

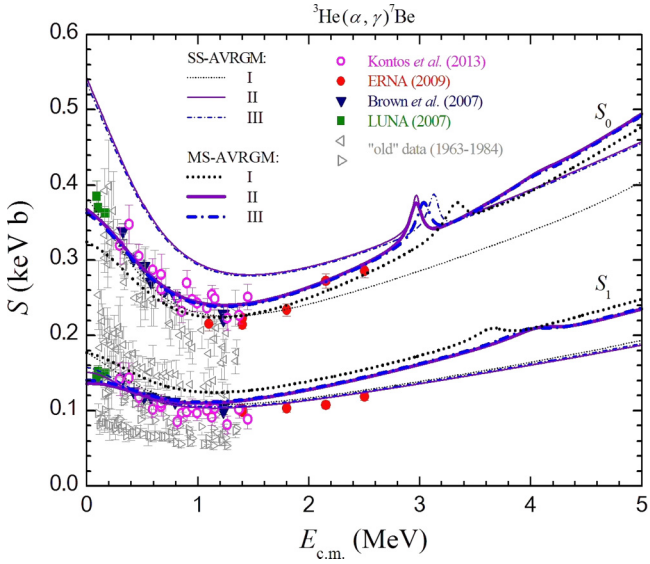

FIG. 15. The ^{3}He$(\alpha,\gamma)^7$Be total astrophysical S factors for captures to the ^{7}Be ground and first excited states.

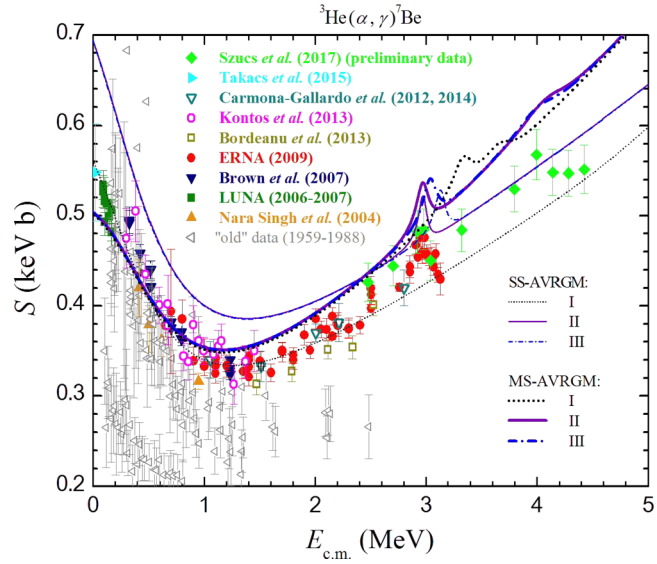

FIG. 16. The total astrophysical S factor for the ^{3}He$(\alpha,\gamma)^7$Be reaction.

MS-AVRGM calculations of the phase shift $\delta_{1/2^-}$ agree very well with the data [50] while the MS-AVRGM calculations of the phase shift $\delta_{3/2^-}$ do slightly worse. Within the SS-AVRGM approach, the calculations of the phase shift $\delta_{1/2^-}$ give adequate description of the data [49], but the calculations of the phase shift $\delta_{3/2^-}$ are underestimated in comparison with the data from that work. For the ^{4}He + ^{3}He scattering, the MS-AVRGM calculations of the p-wave phase shifts $\delta_{1/2^-}$ and $\delta_{3/2^-}$ are in a good agreement with the data and provide a better description than the SS-AVRGM ones. The data [47] on $\delta_{1/2^-}$ and $\delta_{3/2^-}$ lie higher than the other data and our curves as in the case of the s-wave phase shift $\delta_{1/2^+}$. The data on the d-wave phase shifts $\delta_{3/2^+}$ and $\delta_{5/2^+}$ presented, respectively, in Figs. 7 and 8 for ^{4}He + ^{3}H and in Figs. 9 and 10 for ^{4}He + ^{3}He are predominantly concentrated in vicinity of 0^0 with a large scatter for both the systems. In these figures, the calculated d-wave phase shifts lie close enough to the data at low and intermediate energies.

MS-AVRGM calculations II and III for the phase shifts discussed above are almost indistinguishable in the figures. The same situation is in the case of the SS-AVRGM ones. Moreover, the s- and d-wave phase shifts obtained from MS-AVRGM calculation I also turn out to be almost identical to those from MS-AVRGM calculations II and III. The considered phase shifts obtained from SS-AVRGM calculations II and III differ from those of SS-AVRGM calculation I and on the whole describe the data slightly better.

Let us discuss in more detail the f-wave nuclear phase shifts shown in Figs. 11 and 12 for ^{4}He + ^{3}H and in Figs. 13 and 14 for ^{4}He + ^{3}He. SS- and MS-AVRGM calculations I give the positions of the lowest $7/2^-$ and $5/2^-$ resonance states shifted in comparison with their experimental values [53] both for ^{7}Li and for ^{7}Be. For this reason, SS- and MS-AVRGM calculations II and III were done. Energies (E_r) and widths (Γ) of the considered resonances obtained from all these calculations and from the experiments [53] are given in Table III. The energies of the $7/2^-$ and $5/2^-$ resonances from SS-AVRGM calculation I are overestimated for both the systems. As to MS-AVRGM calculation I, the $7/2^-$ resonance energies are also overestimated whereas the $5/2^-$ ones are underestimated. SS- and MS-AVRGM calculations II (III) reproduce the $7/2^-$ resonance energy for the ^{7}Be (^{7}Li) system and give very good description of the data on the phase shift $\delta_{7/2^-}$. The obtained curves lie very close to each other. Furthermore, MS-AVRGM calculations II and III improve the description for the $5/2^-$ resonance position together with the data on the phase shift $\delta_{5/2^-}$ of the ^{4}He + ^{3}He and ^{4}He + ^{3}H scattering as compared with MS-AVRGM calculation I. However, SS-AVRGM calculations II and III make worse the relative description as compared to SS-AVRGM calculation I.

TABLE IV. The breakup thresholds (in MeV) for the ^{7}Li and ^{7}Be ground and first excited states.

Nucleus	Quantity	Experiment	SS-AVRGM			MS-AVRGM		
			I	II	III	I	II	III
^{7}Li	ε_0	2.467	1.672	2.359	2.332	2.467	2.490	2.469
	ε_1	1.989	1.546	1.337	1.376	1.989	2.077	2.115
^{7}Be	ε_0	1.586	0.828	1.481	1.456	1.586	1.714	1.694
	ε_1	1.157	0.710	0.520	0.556	1.157	0.962	0.987

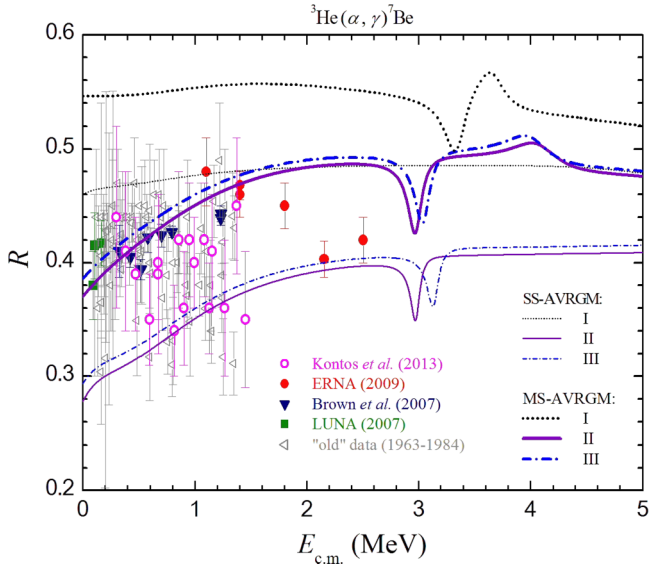

FIG. 17. The branching ratio for the ^{3}He$(\alpha,\gamma)^7$Be reaction.

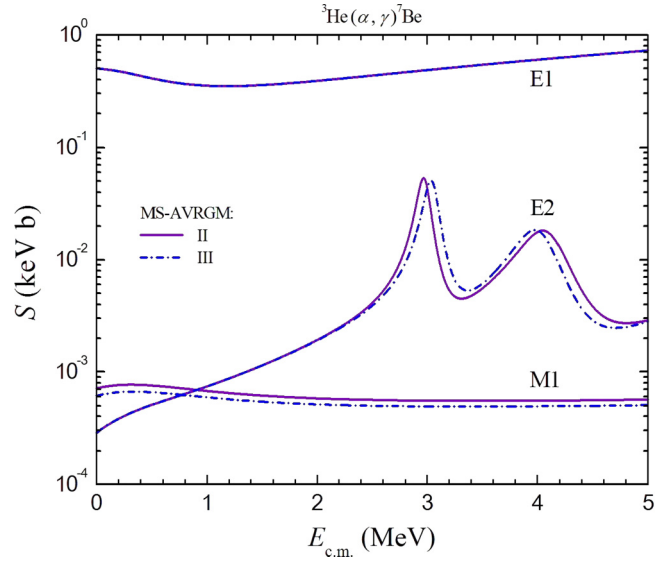

FIG. 18. The ^{3}He$(\alpha,\gamma)^7$Be total astrophysical S factors for the E1, E2, and M1 captures calculated within the MS-AVRGM approach.

SS- and MS-AVRGM calculations III of the ^{4}He + ^{3}He and ^{4}He + ^{3}H f-wave phase shifts are similar enough to SS- and MS-AVRGM calculations II, respectively.

As concerns the AVRGM calculations of the resonance widths, their values are sensitive to the resonance positions. When the calculated resonance positions either coincide with the experimental ones or lie close enough to them, the calculated widths also appear to be in an agreement with the experimental data. This suggestion is clearly seen from Table III.

It is worthwhile to mention that the *ab initio* description of the resonance states for the ^{7}Li and ^{7}Be nuclei in Ref. [24] also meets some difficulties, which are partly similar to those of our microscopic MS-AVRGM calculation I. For example, the lowest $7/2^-$ and $5/2^-$ resonance energies for both the systems from the *ab initio* calculation [24] turn out to be shifted, namely, the $7/2^-$ resonance energy is overestimated in comparison with the experimental one while the $5/2^-$ resonance energy is underestimated. To avoid the problems, authors of that work had to introduce adjustable parameters.

C. The ^{3}He$(\alpha,\gamma)^7$Be radiative capture

Let us consider the radiative capture in the ^{4}He + ^{3}He system, i.e., the ^{3}He$(\alpha,\gamma)^7$Be reaction. The calculated total astrophysical S factors for captures to the ground (S_0) and first excited (S_1) states of ^{7}Be and related experimental data extracted from direct measurements [33,54–61] are shown in Fig. 15. References [54–58] are the so-called "old" data, and Refs. [33,59–61] are the modern ones. SS- and MS-AVRGM calculations I actually generalize our previous calculations [8]. In the present work, we cover significantly larger energy range and take into account the E2 and M1 captures. SS-AVRGM calculation I of the astrophysical S_0 and S_1 factors describes the modern data well. The MS-AVRGM one does slightly worse but reproduces the breakup thresholds for the ^{7}Be ground and first excited states. The breakup thresholds obtained from all the AVRGM calculations and from the experiments [53] are given in Table IV. As it has been demonstrated in the previous subsection, the $7/2^-$ and $5/2^-$ resonance energies turn out to be shifted in AVRGM calculations I. MS-AVRGM calculations II and III improve the description of the modern data on the astrophysical S_0 and S_1 factors but slightly shift the breakup thresholds. An advantage of the former is the capability of reproducing the $7/2^-$ resonance energy (see Table III). SS-AVRGM calculation II also

TABLE V. Zero-energy astrophysical S-factor values $S(0)$ (in keV b) and ratios (in MeV^{-1}) of zero-energy derivative values $S'(0)$ of the astrophysical S factors to the $S(0)$ values for the ^{3}H$(\alpha,\gamma)^7$Li and ^{3}He$(\alpha,\gamma)^7$Be reactions obtained by extrapolating the total astrophysical S factors calculated within the AVRGM.

Reaction	Quantity	SS-AVRGM			MS-AVRGM		
		I	II	III	I	II	III
^{3}H$(\alpha,\gamma)^7$Li	$S(0)$	0.111	0.132	0.132	0.092	0.095	0.095
	$S'(0)/S(0)$	−1.188	−1.160	−1.162	−0.955	−0.920	−0.921
^{3}He$(\alpha,\gamma)^7$Be	$S(0)$	0.561	0.694	0.694	0.502	0.504	0.504
	$S'(0)/S(0)$	−0.524	−0.513	−0.534	−0.225	−0.208	−0.209

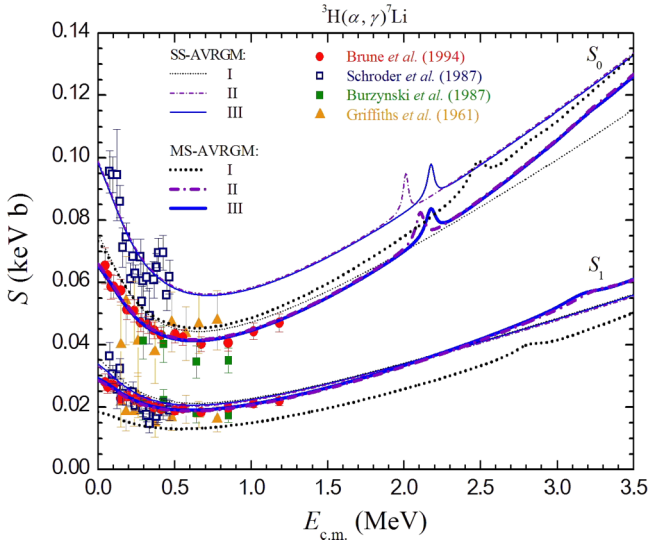

FIG. 19. The ^{3}H(α, γ)^{7}Li total astrophysical S factors for captures to the ^{7}Li ground and first excited states.

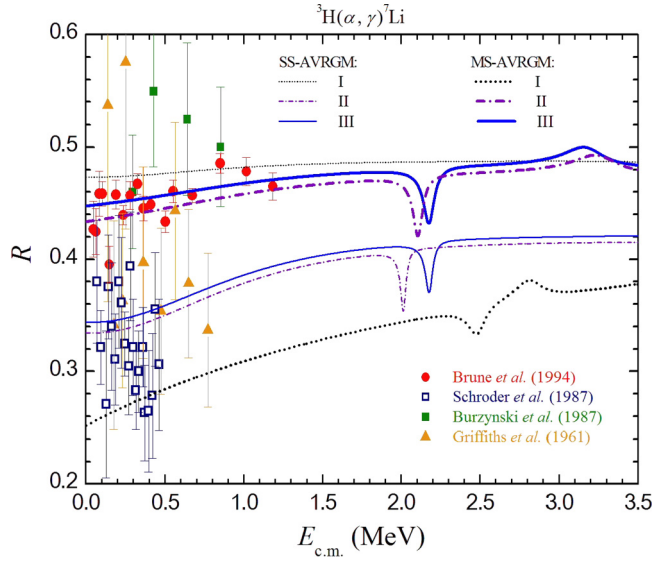

FIG. 21. The branching ratio for the ^{3}H(α, γ)^{7}Li reaction.

reproduces the $7/2^-$ resonance energy but is overestimated compared to the modern data on the astrophysical S_0 factor.

The calculated total astrophysical S factor together with experimental data [21,22,33,54–71] (Refs. [21,22,33,59–61,65–71] are the modern data, and the rest are the "old" ones) and the calculated branching ratio along with the data from the direct measurements [33,54–61] for the ^{3}He(α, γ)^{7}Be reaction are depicted in Figs. 16 and 17, respectively. Extrapolations at zero collision energy of the calculated total astrophysical S factor are presented in Table V. At low energies, the MS-AVRGM calculations of the total astrophysical S factor are very similar to each other and describe the modern data well enough. The main differences arise in vicinities of the peaks corresponding to the $7/2^-$ and $5/2^-$ resonances. The position of the former peak in the energy dependence obtained from MS-AVRGM calculation II coincide with that from the experimental data but calculated values of the total astrophysical S factor lie slightly higher. SS-AVRGM calculation I describes the modern data very well up to vicinity of the first peak. However, the position of this peak is significantly shifted in the calculated energy dependence. SS-AVRGM calculation II reproduces the peak position corresponding to the $7/2^-$ resonance but is considerably overestimated compared to the modern data at very low energies. The main differences between SS-AVRGM calculations II and III are only in the peaks positions. As to the branching ratio, the differences between the AVRGM calculations are more evident. MS-AVRGM calculations II and III describe adequately the modern data on the branching

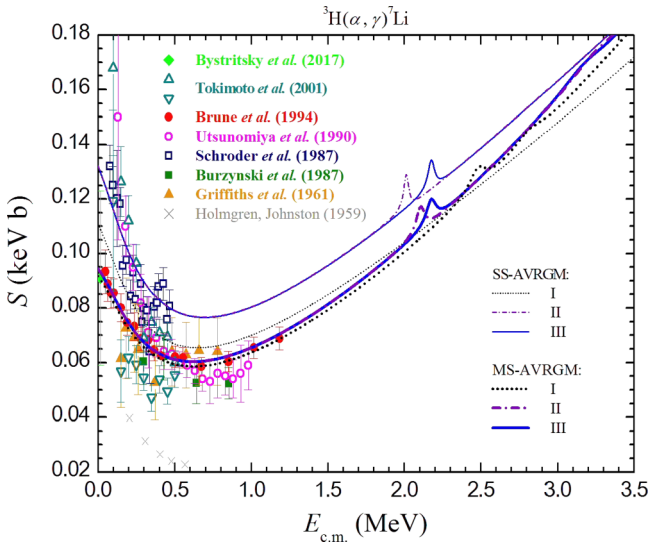

FIG. 20. The total astrophysical S factor for the ^{3}H(α, γ)^{7}Li reaction.

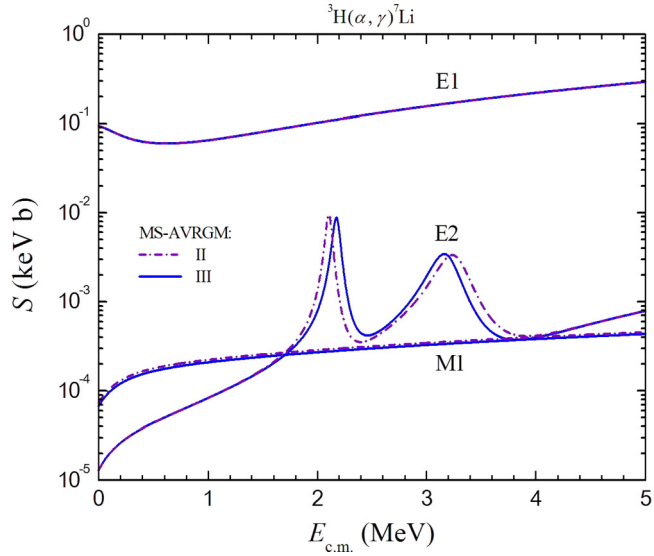

FIG. 22. The ^{3}H(α, γ)^{7}Li total astrophysical S factors for the E1, E2, and M1 captures calculated within the MS-AVRGM approach.

ratio while SS-AVRGM calculations II and III lie slightly lower.

The E1, E2, and M1 capture contributions to the energy dependence of the total astrophysical S factor for ^{3}He$(\alpha,\gamma)^7$Be obtained from MS-AVRGM calculations II and III are drawn in Fig. 18. These calculations give almost identical result for the E1 contribution but their results differ from each other both for the E2 contribution and for the M1 one. The E1 capture contribution plays the dominating role over the whole energy range. In particular, it is in accordance with results of Refs. [24,28,29,72]. The E2 capture from the $7/2^-$ partial wave of the ^{4}He + ^{3}He scattering state to the ^{7}Be ground state is responsible for formation of the first peak in the energy dependence. In turn, the E2 captures from the $5/2^-$ partial wave to the ^{7}Be ground and first excited states provide formation of the second peak. The M1 captures are negligible at the considered energies.

D. The ^{3}H$(\alpha,\gamma)^7$Li radiative capture

In the case of the ^{3}H$(\alpha,\gamma)^7$Li reaction, energy dependences obtained in the framework of the AVRGM are depicted along with experimental data in Fig. 19 for the astrophysical S_0 and S_1 factors, in Fig. 20 for the total astrophysical S factor, and in Fig. 21 for the branching ratio. The total astrophysical S-factor data are taken from works [20,62,73–78]. The data on the astrophysical S_0 and S_1 factors and on the branching ratio are extracted from the direct measurements [73–75,77]. The E1, E2, and M1 contributions to the ^{3}H$(\alpha,\gamma)^7$Li total astrophysical S factor obtained by MS-AVRGM calculations II and III are demonstrated in Fig. 22. The calculated total astrophysical S factor extrapolated at zero collision energy is presented in Table V.

SS- and MS-AVRGM calculations I for the ^{3}H$(\alpha,\gamma)^7$Li astrophysical S_0 and S_1 factors provide only reasonable but not perfect description of the data, especially those from Ref. [77]. Nevertheless, MS-AVRGM calculation I reproduces the breakup thresholds for the ^{7}Li bound states. MS-AVRGM calculations II and III slightly shift these breakup thresholds but allow one to achieve a perfect description of the data [77]. In addition, the $7/2^-$ resonance energy resulting from MS-AVRGM calculation III coincides with its experimental value (see Table III). All the calculated breakup thresholds for ^{7}Li and their experimental values [53] are presented in Table IV. SS-AVRGM calculations II and III make a reasonable enough description of the astrophysical S_1-factor data [77] but significantly exceed the data on the astrophysical S_0 factor from that work. At the same time, the astrophysical S_0- and S_1-factor data from Ref. [75] are simultaneously described well.

All the MS-AVRGM calculations provide a perfect description of the data [77] on the ^{3}H$(\alpha,\gamma)^7$Li total astrophysical S factor. Despite lack of the experimental data in vicinity of the $7/2^-$ resonance energy, MS-AVRGM calculation III is supposed to reproduce the peak position at the corresponding energy in the real energy dependence. The same can be said about SS-AVRGM calculation III, which by the way describes the data [75] rather well. Most likely, only experiments can determine which of these calculations is better for a quantitative description of the peak. MS-AVRGM calculations II and III of the total astrophysical S factor are almost identical at all energies, excepting vicinities of the peaks at the $7/2^-$ and $5/2^-$ resonance energies. The similar situation is in the case of SS-AVRGM calculations II and III. For the branching ratio, AVRGM calculations II and III have quite evident differences. Nevertheless, MS-AVRGM calculations II and III give a good description of the data [77] on the ^{3}H$(\alpha,\gamma)^7$Li branching ratio whereas the SS-AVRGM ones do well for the data [75].

The general statements about the contributions of the E1, E2, and M1 captures to the ^{3}H$(\alpha,\gamma)^7$Be total astrophysical S factor done in the previous subsection remain correct in the case of the considered mirror reaction. However, the quantitative behavior of these contributions is obviously different for the reactions.

TABLE VI. The rms nuclear radii and the electromagnetic properties of ^{7}Li and ^{7}Be in the framework of the AVRGM. The results are obtained assuming the nucleons to be the point-like objects.

Nucleus	Quantity	SS-AVRGM			MS-AVRGM		
		I	II	III	I	II	III
^{7}Li	r_c (fm)	2.235	2.157	2.160	2.190	2.170	2.172
	r_n (fm)	2.301	2.214	2.217	2.232	2.211	2.213
	r_m (fm)	2.273	2.189	2.192	2.214	2.194	2.196
	Q (e fm^2)	−3.921	−3.492	−3.507	−3.325	−3.248	−3.257
	μ (μ_N)	3.1597	3.1563	3.1565	3.1500	3.1496	3.1497
	B(E2) (e^2 fm^4)	7.857	7.249	7.236	5.485	5.628	5.616
	B(M1) (μ_N^2)	2.167	2.134	2.138	2.172	2.170	2.171
^{7}Be	r_c (fm)	2.363	2.254	2.258	2.268	2.258	2.260
	r_n (fm)	2.293	2.194	2.197	2.222	2.214	2.216
	r_m (fm)	2.333	2.228	2.232	2.248	2.239	2.241
	Q (e fm^2)	−6.538	−5.748	−5.774	−5.541	−5.464	−5.480
	μ (μ_N)	−1.2814	−1.2776	−1.2778	−1.2711	−1.2705	−1.2706
	B(E2) (e^2 fm^4)	21.935	19.867	19.830	16.423	16.528	16.522
	B(M1) (μ_N^2)	1.580	1.551	1.555	1.510	1.497	1.499

TABLE VII. The rms nuclear radii of ^{7}Li obtained in previous works.

Authors, reference	Year	Method	Quantity, value
			r_c (fm)
		Experiment	
Suelzle *et al.* [79]	1967	MDAHO	2.39 ± 0.03
Van Niftrik *et al.* [80]	1971	MDAHO	2.55 ± 0.07
Bumiller *et al.* [81]	1972	MIA	2.35 ± 0.10
		MDAHO	2.29 ± 0.04
Gibson *et al.* [82]	1982	MDAHO	2.39
Tanihata *et al.* [83]	1985	MDAHO	2.43 ± 0.03
Tanihata *et al.* [84]	1988	MDAHO	2.27 ± 0.02
			2.40 ± 0.02
		Theory	
Kanada *et al.* [85]	1980	RGM	2.44
Kajino *et al.* [86]	1984	RGM	2.35, 2.51, 2.55, 2.80
Kajino *et al.* [87]	1984	RGM	2.35, 2.55, 2.57
Walliser, Fliessbach [88]	1985	ECM	2.46, 2.47
Buck *et al.* [89]	1985	PCM	2.42 ± 0.04
Kajino [29]	1986	RGM	2.15, 2.35, 2.39, 2.43, 2.44, 2.55, 2.56
Mertelmeier, Hofmann [90]	1986	RGM	2.27, 2.31, 2.38
Buck, Merchant [91]	1988	PCM	2.43 ± 0.02
Nollett [72]	2001	VMC	2.30 ± 0.01
Neff [92]	2011	FMD	2.46
Dohet-Eraly *et al.* [24]	2016	NCSM	2.21
		NCSMC	2.42
			r_n (fm)
		Experiment	
Gibson *et al.* [82]	1982	MDAHO	2.5
Tanihata *et al.* [83]	1985	MDAHO	2.54 ± 0.03
Tanihata *et al.* [84]	1988	MDAHO	2.38 ± 0.02
		Theory	
Kajino *et al.* [86]	1984	RGM	2.35, 2.51, 2.57, 2.83
Kajino *et al.* [87]	1984	RGM	2.34, 2.35, 2.57, 2.59
			r_m (fm)
		Experiment	
Tanihata *et al.* [83]	1985	MDAHO, MDAG	2.50 ± 0.03
Tanihata *et al.* [84]	1988	MDAHO	2.33 ± 0.02
		MDAG	2.35 ± 0.03
		Theory	
Mertelmeier, Hofmann [90]	1986	RGM	2.34, 2.40, 2.46
Csótó, Langanke [93]	2000	RGM	2.28, 2.31, 2.36, 2.39, 2.46, 2.48, 2.50, 2.55

TABLE VIII. The ^{7}Li electromagnetic moments from preceding investigations.

Authors, reference	Year	Method	Quantity, value
			Q (e fm^2)
Combination of calculation (calc.) with experimental data (exp.) from ^{7}Li *atomic (molecular) spectroscopy*			
Kahalas, Nesbet [94]	1963	calc. [94] + exp. [95]	−4.44
Wharton *et al.* [96]	1964	exp. [96] + calc. [94]	−4.50 ± 0.45
Browne, Matsen [97]	1964	calc. [97] + exp. [95]	−4.3
Cade, Huo [98]	1967	calc. [98] + exp. [96]	−3.43[a]
Bender, Davidson [101]	1969	calc. [101] + exp. [96]	−4.3[a]
Lu, Present [102]	1970	calc. [102] + exp. [95]	−4.3 ± 0.3
Green [99]	1971	calc. [99] + exp. [96]	−3.66 ± 0.03
Orth *et al.* [103]	1975	exp. [103] + calc. [104]	−4.125
		exp. [103] + calc. [105]	−4.054
		exp. [103] + calc. [106]	−4.125
		averaging	−4.1 ± 0.6
Garpman *et al.* [106]	1975	calc. [106] + exp. [103]	−4.1 ± 0.5
Nagourney *et al.* [107]	1978	exp. [107] + calc. [106]	−5.9 ± 0.8
Sundholm *et al.* [108]	1984	calc. [108] + exp. [109]	−4.06
Diercksen *et al.* [110]	1988	calc. [110] + exp. [111]	−4.055 ± 0.080
Analysis of experimental data (exp.) on nuclear scattering and their reanalysis (rean.)			
Suelzle *et al.* [79]	1967	exp.	|4.20 ± 0.25|
Van Niftrik *et al.* [80]	1971	exp.	|3.8 ± 1.1|
Bamberger *et al.* [112]	1972	exp.	−1 ± 2
Egelhof *et al.* [113]	1980	exp.	−3.4 ± 0.6
Vermeer *et al.* [114]	1984	exp.	−4.0 ± 1.1
Weller *et al.* [115]	1985	exp.	−3.70 ± 0.08
Barker *et al.* [116]	1989	rean. of exp.	−4.06 ± 0.08
Grawert, Derner [117]	1989	rean. of exp.	−3.84 ± 0.15
			−3.63 ± 0.12
			−3.82 ± 0.15
Voelk, Fick [100]	1991	rean. of exp.	−4.00 ± 0.06
		Theory	
Kanada *et al.* [85]	1980	RGM	−3.70
Bouten, Bouten [118]	1981	HF	−3.62
Kajino *et al.* [86]	1984	RGM	−3.50, −4.39, −4.41, −4.58
Kajino *et al.* [87]	1984	RGM	−3.50, −3.55, −4.38, −4.39, −4.41
Walliser, Fliessbach [88]	1985	ECM	−3.85
Buck *et al.* [89]	1985	PCM	−3.74 ± 0.08
Kajino [29]	1986	RGM	−2.13, −3.50, −3.70, −3.71, −3.73, −4.38, −4.41
Mertelmeier, Hofmann [90]	1986	RGM	−3.42, −3.71, −4.19
Buck, Merchant [91]	1988	PCM	−3.83 ± 0.13
Csótó, Langanke [93]	2000	RGM	−3.51, −3.52, −3.73, −3.75, −3.77, −3.78, −3.80, −3.83
Nollett [72]	2001	VMC	−3.7 ± 0.2
Neff [92]	2011	FMD	−3.91
Dohet-Eraly *et al.* [24]	2016	NCSM	−2.67
		NCSMC	−3.72
			μ (μ_N)
Lutz [119]	1967	exp.	3.256
Van Niftrik *et al.* [80]	1971	exp.	3.2 ± 0.4
Raghavan [120]	1989	exp.	3.256[b]
		Theory	
Bouten, Bouten [118]	1981	HF	3.22
Walliser *et al.* [122]	1983	RGM	3.148

TABLE VIII. (*Continued.*)

Authors, reference	Year	Method	Quantity, value
			μ (μ_N)
Kajino *et al.* [86]	1984	RGM	3.14, 3.15, 3.16
Kajino *et al.* [87]	1984	RGM	3.15, 3.16
Walliser, Fliessbach [88]	1985	ECM	3.20, 3.38
Buck *et al.* [89]	1985	PCM	3.384
Mertelmeier, Hofmann [90]	1986	RGM	2.79, 3.16
Dohet-Eraly *et al.* [24]	2016	NCSM	3.00
		NCSMC	3.02

[a]This value could be obtained by combining the corresponding calculation with the experimental data from Ref. [96] (see, for example, Refs. [99,100]).
[b]This value was obtained in Ref. [120], using experimental data [121].

TABLE IX. The ^{7}Li reduced transition probabilities from preceding investigations.

Authors, reference	Year	Method	Quantity, value
			B(E2) (e^2 fm^4)
Stelson, McGowan [123]	1960	exp.	7.3 ± 1.5
Ritter *et al.* [124]	1962	exp.	7.6 ± 1.1
Van Niftrik *et al.* [80]	1971	exp.	7 ± 4
Bamberger *et al.* [112]	1972	exp.	7.4 ± 0.1
Häusser *et al.* [125]	1973	exp.	8.3 ± 0.6
Vermeer *et al.* [114]	1984	exp.	7.42 ± 0.14
Weller *et al.* [115]	1985	exp.	8.3 ± 0.5
Kajino *et al.* [126]	1988	rean. of exp.	8.9
Vermeer *et al.* [127]	1989	rean. of exp.	7.59 ± 0.10
Barker *et al.* [116]	1989	rean. of exp.	7.59 ± 0.10
Grawert, Derner [117]	1989	rean. of exp.	9.7 ± 1.6
			8.0 ± 1.3
			7.3 ± 1.2
Voelk, Fick [100]	1991	rean. of exp.	7.27 ± 0.12
		Theory	
Bouten, Bouten [118]	1981	HF	6.26
Walliser *et al.* [122]	1983	RGM	7.55
Kajino *et al.* [86]	1984	RGM	6.61, 10.42, 10.57, 11.64
Kajino *et al.* [87]	1984	RGM	6.61, 6.77, 10.33, 10.47, 10.57
Walliser, Fliessbach [88]	1985	ECM	8.04
Buck *et al.* [89]	1985	PCM	7.0 ± 0.3
Kajino [29]	1986	RGM	2.46, 6.61, 7.40, 7.46, 7.55, 10.27, 10.57
Mertelmeier, Hofmann [90]	1986	RGM	5.38, 6.86, 8.49, 11.3
Buck, Merchant [91]	1988	PCM	7.75 ± 0.50
			B(M1) (μ_N^2)
Van Niftrik *et al.* [80]	1971	exp.	2.48 ± 0.12
		Theory	
Bouten, Bouten [118]	1981	HF	2.185
Walliser *et al.* [122]	1983	RGM	2.17
Kajino *et al.* [86]	1984	RGM	2.16, 2.17, 2.34
Kajino *et al.* [87]	1984	RGM	2.16, 2.17
Walliser, Fliessbach [88]	1985	ECM	2.13, 2.45
Buck *et al.* [89]	1985	PCM	2.45
Mertelmeier, Hofmann [90]	1986	RGM	1.96, 2.10, 2.15, 2.17

TABLE X. The rms nuclear radii of ^{7}Be obtained in previous works.

Authors, reference	Year	Method	Quantity, value
			r_c (fm)
		Experiment	
Tanihata *et al.* [83]	1985	MDAHO	2.52 ± 0.03
Tanihata *et al.* [84]	1988	MDAHO	2.36 ± 0.02
Nörtershäuser *et al.* [128]	2009	MIA	2.647 ± 0.017
		Theory	
Kajino *et al.* [86]	1984	RGM	2.65, 2.74
Mertelmeier, Hofmann [90]	1986	RGM	2.39
Nollett [72]	2001	VMC	2.41 ± 0.01
Mason *et al.* [31]	2009	DM	2.52
Neff [92]	2011	FMD	2.67
Dohet-Eraly *et al.* [24]	2016	NCSM	2.375
		NCSMC	2.62
			r_n (fm)
		Experiment	
Tanihata *et al.* [83]	1985	MDAHO	2.41 ± 0.03
Tanihata *et al.* [84]	1988	MDAHO	2.25 ± 0.02
		Theory	
Kajino *et al.* [86]	1984	RGM	2.40, 2.50
			r_m (fm)
		Experiment	
Tanihata *et al.* [83]	1985	MDAHO, MDAG	2.48 ± 0.03
Tanihata *et al.* [84]	1988	MDAHO	2.31 ± 0.02
		MDAG	2.33 ± 0.02
		Theory	
Mertelmeier, Hofmann [90]	1986	RGM	2.34
Csótó, Langanke [93]	2000	RGM	2.36, 2.43, 2.44, 2.51, 2.54, 2.55, 2.56, 2.62
Mason *et al.* [31]	2009	DM	2.48

E. The ^{7}Li and ^{7}Be electromagnetic properties and nuclear radii

The important electromagnetic properties of the ^{7}Li and ^{7}Be nuclei, such as the electric quadrupole (Q) and magnetic dipole (μ) moments of the ground state and the reduced probabilities of E2 (B(E2)) and M1 (B(M1)) transitions from the ground state to the first excited one, as well as the root-mean-square (rms) radii for the charge (r_c), neutron matter (r_n), and nucleon matter (r_m) density distributions in the ground state are also considered in the present work. The calculation of these quantities and a further comparison with available data are the components of a useful test of the approach reliability. Values of the considered quantities calculated within the AVRGM are presented in Table VI for both the nuclei. Related experimental data, estimations, and other calculations known to us at the present time are collected in Tables VII–IX for ^{7}Li and in Tables X and XI for ^{7}Be. In these tables, the following abbreviations are introduced: MDAHO/MDAG is the model-dependent analysis of experimental data based on the harmonic-oscillator/Gaussian distribution of nucleons, MIA is the model-independent analysis of experimental data, ECM is the elementary cluster model, PCM is the potential cluster model, VMC is the variational Monte-Carlo method, FMD is the fermionic molecular dynamics, NCSM is the no-core shell model, DM is the dicluster model, HF is the Hartree-Fock method.

Many experimental data on the rms radii both for ^{7}Li (see Table VII) and for ^{7}Be (see Table X) were extracted by assuming some model distribution of nucleons. There were usually supposed that the density of nucleon distribution had the harmonic-oscillator form. Nevertheless, there are also the model-independent extractions of the rms charge radius r_c. Most theoretical calculations provide the charge radius solely, probably, because its experimental values used for comparison were obtained more reliably than values for the rms matter radii r_n and r_m.

As it can be seen from Tables VIII and IX , the studies of the electric quadrupole moment Q and the reduced transition probability B(E2) for ^{7}Li have a long story. Among them, there are the experimental measurements, their analyses and reanalyses, as well as the theoretical calculations. In the ^{7}Be case (see Table XI), a number of the investigations is much lesser than for ^{7}Li, and experimental data on Q and B(E2) are quite absent. As to the magnetic dipole moment μ and the reduced transition probability B(M1), they were investigated equally for both the nuclei but more poorly than, for example, Q and B(E2) for ^{7}Li.

The quantities discussed in this subsection were calculated within the various models (see Tables VII–XI). The results of those calculations reveal a certain scatter but, on the whole, most of them are close to the experimental ones, which in

TABLE XI. The ^{7}Be electromagnetic properties from preceding investigations.

Authors, reference	Year	Method	Quantity, value
			Q (e fm^2)
		Theory	
Kajino *et al.* [86]	1984	RGM	−4.89, −5.51
Mertelmeier, Hofmann [90]	1986	RGM	−5.84
Csótó, Langanke [93]	2000	RGM	−6.22, −6.27, −6.40, −6.61, −6.64,−7.23, −7.28, −7.41
Nollett [72]	2001	VMC	-5.9 ± 0.3
Mason *et al.* [31]	2009	DM	−4.79
Neff [92]	2011	FMD	−6.83
Dohet-Eraly *et al.* [24]	2016	NCSM	−4.57
		NCSMC	−6.14
			μ (μ_N)
Kappertz *et al.* [129]	1998	exp.	-1.398 ± 0.015
Nörtershäuser *et al.* [128]	2009	exp.	-1.3995 ± 0.0005
		Theory	
Kajino *et al.* [86]	1984	RGM	−1.27, −1.28
Buck *et al.* [89]	1985	PCM	−1.533
Mertelmeier, Hofmann [90]	1986	RGM	−1.27
Mason *et al.* [31]	2009	DM	−1.53
Dohet-Eraly *et al.* [24]	2016	NCSM	−1.14
		NCSMC	−1.16
			B(E2) (e^2 fm^4)
		Theory	
Walliser *et al.* [122]	1983	RGM	21.76
Kajino *et al.* [86]	1984	RGM	22.7, 29.2
Mertelmeier, Hofmann [90]	1986	RGM	17.0
Mason *et al.* [31]	2009	DM	18.3
			B(M1) (μ_N^2)
Ajzenberg-Selove [130]	1979	exp.	1.87 ± 0.25[a]
		Theory	
Walliser *et al.* [122]	1983	RGM	1.58
Kajino *et al.* [86]	1984	RGM	1.58
Buck *et al.* [89]	1985	PCM	1.87
Kajino [29]	1986	RGM	1.59
Mertelmeier, Hofmann [90]	1986	RGM	1.58
Mason *et al.* [31]	2009	DM	1.86

[a]This value could be obtained by using experimental data given in Ref. [130] (see, for example, Refs. [90,122]).

turn lie rather close to each other. Finally, our results presented in Table VI could be also characterized in the similar manner.

IV. CONCLUSION

In the present work, the microscopic study of the mirror radiative capture reactions ^{3}H$(\alpha,\gamma)^7$Li and ^{3}He$(\alpha,\gamma)^7$Be has been performed in the framework of the AVRGM. The considered wide energy region covered not only the low energies but also the intermediate ones including the lowest resonances of the ^{7}Li and ^{7}Be nuclei. Along with the dominating E1 transitions, the E2 and M1 ones have been taken into consideration. The ^{3}He$(\alpha,\gamma)^7$Be total astrophysical S factor calculated within the MS-AVRGM approach agrees reasonably well with the modern data in the range from the low energies up to vicinity of the $7/2^-$ resonance of ^{7}Be. MS-AVRGM calculations II and III have visible differences in vicinities of the resonances only. The former gives the exact $7/2^-$ resonance position whereas the latter slightly shifts this position in the energy dependence. In both the calculations, the total astrophysical S factors for the captures to the ^{7}Be ground and first excited states and the ^{3}He$(\alpha,\gamma)^7$Be branching ratio describe sufficiently well the data from the modern direct measurements. The ^{3}H$(\alpha,\gamma)^7$Li total astrophysical S factor calculated within the MS-AVRGM approach is in a perfect agreement with the data both from Ref. [77] and from the recent work [20]. MS-AVRGM calculation II slightly shifts the $7/2^-$ resonance position while MS-AVRGM calculation III reproduces it. The total astrophysical S factors for the captures to the ^{7}Li ground and first excited states and the corresponding branching ratio also agree very well with the data [77]. As in the case of the mirror reaction, MS-AVRGM calculations II and III for the ^{3}H$(\alpha,\gamma)^7$Li total astrophysical S factor differ visibly from each other in the resonance vicinities only.

The ^{3}H$(\alpha,\alpha)^3$H and ^{3}He$(\alpha,\alpha)^3$He elastic scattering and the properties of the ^{7}Li and ^{7}Be bound and low-lying resonance states have been also considered within the AVRGM. The ^{3}H$(\alpha,\alpha)^3$H and ^{3}He$(\alpha,\alpha)^3$He s-, p-, and d-wave nuclear phase shifts obtained from MS-AVRGM calculations II and III describe the data rather reasonably. The $7/2^-$ f-wave phase shifts obtained from these calculations also agree with the data rather well. Unfortunately, the calculated positions of the $5/2^-$ resonances turn out to be shifted. That is why the calculated $5/2^-$ f-wave phase shifts provide reasonably only the qualitative description of the data on the ^{3}H$(\alpha,\alpha)^3$H and ^{3}He$(\alpha,\alpha)^3$He scattering while the quantitative description is not good enough. The energy dependences of the s-, p-, and d-wave phase shifts from MS-AVRGM calculation II are almost identical to those from MS-AVRGM calculation III at all considered energies. For the energy dependences of the f-wave phase shifts, the differences arise in vicinities of the resonance positions. As for the ^{7}Li and ^{7}Be properties, the calculated electromagnetic quantities, rms nuclear radii, and breakup thresholds of the ^{7}Li and ^{7}Be bound states are in a good correspondence with the data. Moreover, the energies of the $7/2^-$ resonance states of the ^{7}Be and ^{7}Li nuclei are reproduced within MS-AVRGM calculation II and III, respectively, and the calculated widths of these resonances are in a reasonable agreement with the experimental values.

The developed microscopic SS- and MS-AVRGM approaches are successful in the unified consistent description of the considered reactions in the low-energy region. It was shown in our previous work [8] for the first time. However, the present study demonstrates that the extension of the considered energy range and the data set to be described simultaneously leads to some problems. For example, the ^{3}He$(\alpha,\gamma)^7$Be and ^{3}H$(\alpha,\gamma)^7$Li unified AVRGM treatment reproducing the lowest $7/2^-$ resonance energy of ^{7}Be gives the shifted slightly energy of the analogous resonance of ^{7}Li and vice versa. The simultaneous reproducing the lowest $7/2^-$ resonance energies of ^{7}Li and ^{7}Be is desirable for a perfect description of the corresponding reactions at the intermediate energies. It should be noted that the well-founded *ab initio* description of the considered reactions given in the recent work [24] within the NCSMC approach also met to some extent the similar problems. In particular, the resonance positions obtained in that work without any parameters turned out to be shifted, and their reproducing in fact required introducing adjustable parameters. On the whole, both our microscopic MS-AVRGM approach and that *ab initio* NCSMC one make it possible to describe the wide enough set of the data in the consistent manner and to obtain useful information in the research area.

Descriptive capabilities and a success of any nuclear model depend on different circumstances. One of the most crucial features of a model is the quality of a trial wave function that should incorporate most significant components, which are in fact responsible for the model limitations. Thus, improving this function by an extension of the model space could be considered as a way for developing an approximate approach. As to directions for further development and extension of our approach, there are several lines. The most obvious way is to apply more complicated intrinsic cluster wave functions, for example, with a greater number of the expansion terms. The next one is to take into consideration other cluster channels, including three-cluster configurations. Enriching the trial wave function by polarization terms for better description of the internal region is one more way for improving the developed approach. Finally, the predictive power of the approach can be increased by generalization of its algorithms to cover a wider class of nuclear potentials, in particular, utilized in *ab initio* calculations.

ACKNOWLEDGMENT

The work was supported by the Russian Science Foundation (Project No. 16-12-10048).

APPENDIX A

Expansions over the basis of the eigenfunctions of a three-dimensional harmonic oscillator and cluster aspects of nuclear structure and dynamics serve as starting points of the AVRGM. Cluster representation suggests the following form of the trial many-particle total wave function of a two-cluster system:

$$\Psi = \hat{\mathcal{A}}\{\phi^{(1)}\phi^{(2)}f(\mathbf{q})\}, \tag{A1}$$

where $\hat{\mathcal{A}}$ is the antisymmetrization operator; $\phi^{(1)}$ and $\phi^{(2)}$ are the intrinsic wave functions of the clusters; $f(\mathbf{q})$ is the relative motion wave function; $\mathbf{q}$ is the vector characterizing the relative distance between the clusters. The intrinsic wave functions are usually considered to be fixed, and the problem is reduced to finding $f(\mathbf{q})$. The expansion of $f(\mathbf{q})$ over the oscillator functions

$$f_{\nu lm}(\mathbf{q}) = (-1)^{(\nu-l)/2}\sqrt{\frac{2\,\Gamma\big((\nu-l+2)/2\big)}{r_0^3\,\Gamma\big((\nu+l+3)/2\big)}}\,(q/r_0)^l \times L^{(l+1/2)}_{(\nu-l)/2}\big(q^2/r_0^2\big)\exp\big(-q^2/2\,r_0^2\big)\,Y_{lm}(\mathbf{n_q}), \tag{A2}$$

in which Γ and $L_n^{(\beta)}$ are the gamma-function and the generalized Laguerre polynomial, respectively, and r_0 is the oscillator radius, leads to representation of the total wave function in the form of series

$$\Psi = \sum_{J^\pi M l s \nu} C_{J^\pi M l s \nu}\Psi_{J^\pi M l s \nu} \tag{A3}$$

of the AVRGM basis functions

$$\Psi_{J^\pi M l s \nu} = N_{J^\pi l s \nu}\,\hat{\mathcal{A}}\left\{\sum_{m+\sigma=M} C^{JM}_{lm\;s\sigma}[\phi^{(1)}\phi^{(2)}]_{s\sigma}\,f_{\nu lm}(\mathbf{q})\right\}. \tag{A4}$$

In Eq. (A4), spins of the clusters are coupled to the channel spin s, which is in turn coupled with the orbital angular momentum l to the total angular momentum J; π is the parity depending on the parities of the intrinsic cluster wave functions and the function $f_{\nu lm}$; $N_{J^\pi l s \nu}$ is the normalization. Thus, the problem transforms to determination of the expansion coefficients $C_{J^\pi M l s \nu}$. These coefficients obey an infinite set of linear algebraic equations obtained by projecting

the Schrödinger equation onto the AVRGM basis functions (A4). For the discrete spectrum, the summation in Eq. (A3) can be truncated at a sufficiently large value $\nu = \nu_{\max}$, and a finite set of homogeneous algebraic equations for the expansion coefficients $C^{(\mathrm{D})}_{J^\pi M l s \nu}$ arises:

$$\sum_{l\,s}\sum_{\nu=\nu_0}^{\nu_{\max}} \left(\langle J^\pi M \tilde{l}\tilde{s}\tilde{\nu}|H|J^\pi M l s \nu\rangle - E\,\delta_{\tilde{s}s}\delta_{\tilde{l}l}\delta_{\tilde{\nu}\nu}\right) C^{(\mathrm{D})}_{J^\pi M l s \nu} = 0, \quad \tilde{\nu} = \nu_0,\ \nu_0+2,\ldots,\ \nu_{\max}. \tag{A5}$$

For the continuum, such truncation of the expansion series is not appropriate. It is necessary to take properly into account the asymptotic behavior $C^{(\mathrm{as})}_{J^\pi M l s \nu}$ of the expansion coefficients $C^{(\mathrm{C})}_{J^\pi M l s \nu}$ [8], starting from a sufficiently large value $\nu = \nu_{\mathrm{as}}$. This results in a finite set of inhomogeneous algebraic equations of the following type:

$$\sum_{l\,s}\sum_{\nu=\nu_0}^{\nu_{\mathrm{as}}-2} \left(\langle J^\pi M \tilde{l}\tilde{s}\tilde{\nu}|H|J^\pi M l s \nu\rangle - E\,\delta_{\tilde{s}s}\delta_{\tilde{l}l}\delta_{\tilde{\nu}\nu}\right) C^{(\mathrm{C})}_{J^\pi M l s \nu} = F_{J^\pi M \tilde{l}\tilde{s}\tilde{\nu}}, \quad \tilde{\nu} = \nu_0,\ \nu_0+2,\ldots,\ \nu_{\mathrm{as}}, \tag{A6}$$

$$F_{J^\pi M \tilde{l}\tilde{s}\tilde{\nu}} = -\sum_{l\,s}\sum_{\nu=\nu_{\mathrm{as}}}^{\nu'_{\max}} \langle J^\pi M \tilde{l}\tilde{s}\tilde{\nu}|H|J^\pi M l s \nu\rangle\, C^{(\mathrm{as})}_{J^\pi M l s \nu}. \tag{A7}$$

The matrix elements entering into Eq. (A7) decrease significantly for $\nu \to \infty$ [7], and the contribution of the corresponding terms is negligible. This fact justifies the truncation in Eq. (A7) at some upper limit $\nu = \nu'_{\max}$.

The convergence of the expansion (A3) for discrete spectrum functions that are square-integrable ones is evident. Convergence properties of this expansion for continuum functions, which do not belong to the space of the square-integrable ones, were studied comprehensively in Refs. [131,132], and the pointwise convergence was proved.

The total angular momentum and parity conservation removes the summation over J^π in Eqs. (A5)–(A7). The channel spin of the considered systems has the only one value $s = 1/2$, which ensures the absence of the tensor interaction contribution and hence causes decoupling of the channels with the different orbital angular momentum l. As a result, the single summation over the number of oscillator quanta ν remains in Eqs. (A5)–(A7) for the considered states. Our calculations were performed at different sizes of the AVRGM basis (A4). At the fixed J^π, M, l, and s values, the number of the AVRGM basis functions (A4) involved in the expansions was varied from a few tens up to a thousand. Since numerical procedures and algorithms are elaborated well, so it allows one to use a rather large size of the truncated basis. The numerical calculations of the quantities characterizing the discrete spectrum states demonstrate that it is sufficient to include about a hundred terms in the expansions. As to the continuum, the situation looks more complicated. The radiative capture treatment requires to increase the number of the utilized basis functions (A4). The reliable calculations should take into account at least five hundred terms in the expansions.

APPENDIX B

In this section, the reduced matrix elements of the electric dipole and quadrupole operators and the magnetic dipole one for the mirror seven-nucleon $^4\mathrm{He} + {}^3\mathrm{H}$ and $^4\mathrm{He} + {}^3\mathrm{He}$ systems derived in the framework of the MS-AVRGM approach are presented. The corresponding explicit expressions read

$$\left\langle J^{\pi_f}_f l_f s \nu_f \left\| M^{\mathrm{E}}_1 \right\| J^{\pi_i}_i l_i s \nu_i \right\rangle = e\sqrt{r_{01}r_{02}}\,\zeta\,\frac{\rho^{10}}{14}\sqrt{\frac{3}{\pi}}\,\Theta^{(1)}_{J_f l_f J_i l_i s}\left(\sqrt{\frac{r_{01}}{r_{02}}}\,F^{(1,l_i;1,0)}_{l_f\nu_f l_i\nu_i s} + \sqrt{\frac{r_{02}}{r_{01}}}\,F^{(1,l_f;0,1)}_{l_f\nu_f l_i\nu_i s}\right), \tag{B1}$$

$$\left\langle J^{\pi_f}_f l_f s \nu_f \left\| M^{\mathrm{E}}_2 \right\| J^{\pi_i}_i l_i s \nu_i \right\rangle = e\,r_{02}r_{01}\,\frac{\rho^{11}}{2a_1}\sqrt{\frac{5}{\pi}}\left[a_2\,\Theta^{(2)}_{J_f l_f J_i l_i s}\left(\frac{r_{01}}{r_{02}}\,F^{(1,l_i;2,0)}_{l_f\nu_f l_i\nu_i s} + \frac{r_{02}}{r_{01}}\,F^{(1,l_f;0,2)}_{l_f\nu_f l_i\nu_i s}\right) - \sqrt{30}\sum_l \Omega^{(2,l)}_{J_f l_f J_i l_i s}\,F^{(2,l;1,1)}_{l_f\nu_f l_i\nu_i s}\right], \tag{B2}$$

$$\left\langle J^{\pi_f}_f l_f s \nu_f \left\| M^{\mathrm{M}}_1 \right\| J^{\pi_i}_i l_i s \nu_i \right\rangle = \mu_{\mathrm{N}}\,\frac{\rho^9}{2}\sqrt{\frac{3}{\pi}}\left[g\,\Xi^{(1)}_{J_f l_f J_i l_i s}\,F^{(1,l_f;0,0)}_{l_f\nu_f l_i\nu_i s} - \frac{2\rho}{a_1}\sqrt{6}\sum_l \Omega^{(1,l)}_{J_f l_f J_i l_i s}\,F^{(2,l;1,1)}_{l_f\nu_f l_i\nu_i s}\right]. \tag{B3}$$

Here the following denotations are introduced:

$$\Theta^{(\lambda)}_{J_f l_f J_i l_i s} = (-1)^{J_i+l_f+s+\lambda}\,\Pi_{J_f J_i l_i}\,C^{l_f 0}_{l_i 0\,\lambda 0}\begin{Bmatrix} l_i & s & J_i \\ J_f & \lambda & l_f\end{Bmatrix},$$

$$\Omega^{(\lambda,l)}_{J_f l_f J_i l_i s} = (-1)^{J_i+l_f+s+\lambda}\,\Pi_{J_f l_f J_i l_i}\,C^{l0}_{l_f 0\,10}\,C^{l0}_{l_i 0\,10}\begin{Bmatrix} 1 & \lambda & 1 \\ l_f & l & l_i\end{Bmatrix}\begin{Bmatrix} l_i & s & J_i \\ J_f & \lambda & l_f\end{Bmatrix},$$

$$\Xi^{(\lambda)}_{J_f l_f J_i l_i s} = (-1)^{J_f+l_f+s+\lambda}\,\Pi_{J_f J_i\, s}\,\sqrt{s(s+1)}\;\delta_{l_f l_i}\begin{Bmatrix} s & l_f & J_i \\ J_f & \lambda & s \end{Bmatrix},$$

$$\Pi_{j_1\, j_2 \ldots j_n} = \sqrt{(2j_1+1)(2j_2+1)\ldots(2j_n+1)}\,,$$

$$F^{(k,\,l;\,\lambda_2,\,\lambda_1)}_{l_2 \nu_2\, l_1 \nu_1\, s} = \frac{2\pi}{\kappa_{\nu_2 l_2 s}\,\kappa_{\nu_1 l_1 s}(\nu_2-\lambda_2)!(\nu_1-\lambda_1)!}\,\frac{\partial^{\nu_2-\lambda_2}}{\partial Q^{\nu_2-\lambda_2}}\,\frac{\partial^{\nu_1-\lambda_1}}{\partial R^{\nu_1-\lambda_1}}\int_{-1}^{1} U^{(k)}(Q,R,t)\,P_l(t)\,dt\Big|_{Q=R=0},$$

$$\kappa^2_{\nu l s} = \frac{2\pi}{\nu!}\left[\left(\frac{6}{7}\right)^{\nu} - 3\left(\frac{5}{14}\right)^{\nu} + 3\left(-\frac{1}{7}\right)^{\nu} - \left(-\frac{9}{14}\right)^{\nu}\right]\varepsilon_{\nu l},$$

$$\varepsilon_{\nu l} = \begin{cases} \dfrac{2^{l+1}\nu!((\nu+l)/2)!}{(\nu+l+1)!((\nu-l)/2)!}, & l \leqslant \nu,\ \ l+\nu-\text{even}, \\ 0, & \text{in other cases}, \end{cases}$$

$$U^{(1)}(Q,R,t) \equiv U^{(1)}(\mathbf{Q},\mathbf{R}) = w\,(u-1)^3,$$

$$U^{(2)}(Q,R,t) \equiv U^{(2)}(\mathbf{Q},\mathbf{R}) = w\,(a_2 u + a_3)\,(u-1)^2,$$

$$u = \exp\left(\frac{\rho Q R t}{2}\right), \quad w = \exp\left[\frac{3}{7}\left(\varsigma(Q^2-R^2) - \frac{3}{2}\rho Q R t\right)\right],$$

$$\rho = 2\frac{r_{01}r_{02}}{r_{01}^2+r_{02}^2}, \quad \varsigma = \frac{r_{01}^2-r_{02}^2}{r_{01}^2+r_{02}^2},$$

$$\{a_1,\ a_2,\ a_3\} = \{196,\ 34,\ 15\}, \quad g = g_{\rm p}, \quad \zeta = -1 \quad \text{for the } ^4\text{He} + ^3\text{H system},$$

$$\{a_1,\ a_2,\ a_3\} = \{98,\ 25,\ 24\}, \quad g = g_{\rm n}, \quad \zeta = 1 \quad \text{for the } ^4\text{He} + ^3\text{He system},$$

$\begin{Bmatrix} a & b & c \\ d & e & f \end{Bmatrix}$ is the $6j$ symbol [41], δ_{fi} is the Kronecker symbol, $P_l(t)$ is the Legendre polynomial, and $t = \cos\theta_{\mathbf{QR}}$, $\theta_{\mathbf{QR}}$ is the angle between the vectors $\mathbf{Q}$ and $\mathbf{R}$.

Equations (B1)–(B3) are in fact found by utilizing the generating functions method (see Ref. [8] and references cited therein for details). It should be reminded that the first step of this method includes the calculation of matrix elements between the generating functions for the AVRGM basis [8], the so-called generating matrix elements. For the considered operators, these generating matrix elements have the form

$$\langle \mathbf{Q}, s\sigma_f | M^{\rm E}_{1\mu} | \mathbf{R}, s\sigma_i \rangle = e\sqrt{r_{01}r_{02}}\,\zeta\,\frac{\rho^{10}}{7}\,\delta_{\sigma_f\sigma_i}\,U^{(1)}(\mathbf{Q},\mathbf{R})\big(\tilde{Q}\,Y_{1\mu}(\mathbf{n}_{\tilde{\mathbf{Q}}}) + \tilde{R}\,Y_{1\mu}(\mathbf{n}_{\tilde{\mathbf{R}}})\big), \tag{B4}$$

$$\langle \mathbf{Q}, s\sigma_f | M^{\rm E}_{2\mu} | \mathbf{R}, s\sigma_i \rangle = e\,r_{02}r_{01}\,\frac{\rho^{11}}{a_1}\,\delta_{\sigma_f\sigma_i}\left[U^{(2)}(\mathbf{Q},\mathbf{R})(\tilde{\mathbf{Q}}+\tilde{\mathbf{R}})^2\,Y_{2\mu}(\mathbf{n}_{\tilde{\mathbf{Q}}+\tilde{\mathbf{R}}}) - 49\,\frac{U^{(1)}(\mathbf{Q},\mathbf{R})}{u-1}\,\big(\tilde{Q}^2\,Y_{2\mu}(\mathbf{n}_{\tilde{\mathbf{Q}}}) + \tilde{R}^2\,Y_{2\mu}(\mathbf{n}_{\tilde{\mathbf{R}}})\big)\right], \tag{B5}$$

$$\langle \mathbf{Q}, s\sigma_f | M^{\rm M}_{1\mu} | \mathbf{R}, s\sigma_i \rangle = \mu_{\rm N}\frac{\rho^9}{2}\sqrt{\frac{3}{\pi}}\left(g\sqrt{s(s+1)}\;C^{s\sigma_f}_{s\sigma_i\,1\mu}\;U^{(1)}(\mathbf{Q},\mathbf{R}) - \mathrm{i}\frac{2\rho}{a_1}\,\delta_{\sigma_f\sigma_i}\,U^{(2)}(\mathbf{Q},\mathbf{R})\,[\mathbf{Q}\times\mathbf{R}]_{1\mu}\right), \tag{B6}$$

where σ_i and σ_f are the channel spin projections of the initial and final states, respectively; $\mathbf{R}$ and $\mathbf{Q}$ are the generating parameters related to the scaled ones $\tilde{\mathbf{R}}$ and $\tilde{\mathbf{Q}}$ by

$$\tilde{\mathbf{R}} = \sqrt{\frac{r_{02}}{r_{01}}}\,\mathbf{R}, \quad \tilde{\mathbf{Q}} = \sqrt{\frac{r_{01}}{r_{02}}}\,\mathbf{Q}.$$

The next steps consist in obtaining all the necessary matrix elements between the AVRGM basis functions from the generating matrix elements (B4)–(B6) with the aid of the relation between the AVRGM basis and the generating functions. Finally, the reduced matrix elements (B1)–(B3) are extracted by the Wigner–Eckart theorem (9).

[1] M. Freer, H. Horiuchi, Y. Kanada-En'yo, D. Lee, and U.-G. Meißner, Rev. Mod. Phys. **90**, 035004 (2018).

[2] P. Navrátil, S. Quaglioni, G. Hupin, C. Romero-Redondo, and A. Calci, Phys. Scr. **91**, 053002 (2016).

[3] E. G. Adelberger, A. García, R. G. H. Robertson *et al.*, Rev. Mod. Phys. **83**, 195 (2011).

[4] Y. Xu, K. Takahashi, S. Goriely M. Arnould, M. Ohta, and H. Utsunomiya, Nucl. Phys. A **918**, 61 (2013).

[5] G. F. Filippov and I. P. Okhrimenko, Sov. J. Nucl. Phys. **32**, 480 (1980) [Yad. Fiz. **32**, 932 (1980)].
[6] G. F. Filippov, Sov. J. Nucl. Phys. **33**, 488 (1981) [Yad. Fiz. **33**, 928 (1981)].
[7] I. P. Okhrimenko, Nucl. Phys. A **424**, 121 (1984).
[8] A. S. Solovyev and S. Yu. Igashov, Phys. Rev. C **96**, 064605 (2017).
[9] K. Wildermuth and Y. C. Tang, *A Unified Theory of the Nucleus* (Vieweg, Braunschweig, 1977).
[10] A. S. Solovyev and S. Yu. Igashov, Yad. Fiz. Inzhin. **4**, 989 (2013) (in Russian).
[11] A. S. Solovyev, S. Yu. Igashov, and Yu. M. Tchuvil'sky, Phys. At. Nucl. **77**, 1453 (2014) [Yad. Fiz. **77**, 1525 (2014)].
[12] A. S. Solovyev, S. Yu. Igashov, and Yu. M. Tchuvil'sky, J. Phys. Conf. Ser. **569**, 012020 (2014).
[13] A. S. Solovyev, S. Yu. Igashov, and Yu. M. Tchuvil'sky, Bull. Russ. Acad. Sci. Phys. **78**, 433 (2014) [Izv. RAN. Ser. Fiz. **78**, 621 (2014)].
[14] A. S. Solovyev, S. Yu. Igashov, and Yu. M. Tchuvil'sky, Bull. Russ. Acad. Sci. Phys. **79**, 499 (2015) [Izv. RAN. Ser. Fiz. **79**, 541 (2015)].
[15] A. S. Solovyev, S. Yu. Igashov, and Yu. M. Tchuvil'sky, Eur. Phys. J. Web Conf. **86**, 00054 (2015).
[16] A. S. Solovyev, S. Yu. Igashov, and Yu. M. Tchuvil'sky, Eur. Phys. J. Web Conf. **117**, 09017 (2016).
[17] A. S. Solovyev, S. Yu. Igashov, and Yu. M. Tchuvil'sky, Bull. Russ. Acad. Sci. Phys. **80**, 290 (2016) [Izv. RAN. Ser. Fiz. **80**, 322 (2016)].
[18] A. S. Solovyev, S. Yu. Igashov, and Yu. M. Tchuvil'sky, J. Phys. Conf. Ser. **863**, 012015 (2017).
[19] B. D. Fields, Annu. Rev. Nucl. Part. Sci. **61**, 47 (2011).
[20] V. M. Bystritsky, G. N. Dudkin, E. G. Emets, M. Filipowicz, A. R. Krylov, B. A. Nechaev, A. Nurkin, V. N. Padalko, A. V. Philippov, and A. B. Sadovsky, Phys. Part. Nucl. Lett. **14**, 560 (2017) [Pis'ma Fiz. Elem. Chastits At. Yadra **14**, 366 (2017)].
[21] M. P. Takács, D. Bemmerer, T. Szücs, and K. Zuber, Phys. Rev. D **91**, 123526 (2015).
[22] T. Szücs, G. Gyürky, Z. Halász, G. Gy. Kiss, and Z. Fülöp, Eur. Phys. J. Web Conf. **165**, 01049 (2017).
[23] A. Di Leva, L. Gialanella, and F. Strieder, J. Phys. Conf. Ser. **665**, 012002 (2016).
[24] J. Dohet-Eraly, P. Navrátil, S. Quaglioni, W. Horiuchi, G. Hupin, and F. Raimondi, Phys. Lett. B **757**, 430 (2016).
[25] E. M. Tursunov, S. A. Turakulov, and A. S. Kadyrov, Phys. Rev. C **97**, 035802 (2018).
[26] S. B. Dubovichenko, N. A. Burkova, and A. V. Dzhazairov-Kakhramanov, Indian J. Phys. **93**, 279 (2019).
[27] R. Higa, G. Rupak, and A. Vaghani, Eur. Phys. J. A **54**, 89 (2018).
[28] T. A. Tombrello and P. D. Parker, Phys. Rev. **131**, 2582 (1963).
[29] T. Kajino, Nucl. Phys. A **460**, 559 (1986).
[30] S. B. Dubovichenko and A.V. Dzhazairov-Kakhramanov, Phys. Part. Nucl. **28**, 615 (1997) [Fiz. Elem. Chastits At. Yadra. **28**, 1529 (1997)].
[31] A. Mason, R. Chatterjee, L. Fortunato, and A. Vitturi, Eur. Phys. J. A **39**, 107 (2009).
[32] P. Mohr, Phys. Rev. C **79**, 065804 (2009).
[33] A. Di Leva, L. Gialanella, R. Kunz *et al.*, Phys. Rev. Lett. **102**, 232502 (2009); **103**, 159903(E) (2009).
[34] A. M. Shirokov, G. Papadimitriou, A. I. Mazur, I. A. Mazur, R. Roth, and J. P. Vary, Phys. Rev. Lett. **117**, 182502 (2016).
[35] K. Kravvaris and A. Volya, Phys. Rev. Lett. **119**, 062501 (2017).
[36] R. Wirth, D. Gazda, P. Navrátil, and R. Roth, Phys. Rev. C **97**, 064315 (2018).
[37] V. S. Vasilevsky, Yu. A. Lashko, and G. F. Filippov, Phys. Rev. C **97**, 064605 (2018).
[38] V. S. Vasilevsky, K. Kato, and N. Takibayev, Phys. Rev. C **98**, 024325 (2018).
[39] P. Ring and P. Schuck, *The Nuclear Many-Body Problem* (Springer-Verlag, New York, 1980).
[40] D. Baye and P. Descouvemont, Nucl. Phys. A **407**, 77 (1983).
[41] D. A. Varshalovich, A. N. Moskalev, and V. K. Khersonskii, *Quantum Theory of Angular Momentum* (World Scientific Publishing, Singapore, 1988).
[42] J. M. Blatt and V. F. Weisskopf, *Theoretical Nuclear Physics* (Springer-Verlag, New York, 1979).
[43] S. Gartenhaus and C. Schwartz, Phys. Rev. **108**, 482 (1957).
[44] W. A. Fowler, G. R. Caughlan, and B. A. Zimmerman, Annu. Rev. Astron. Astrophys. **5**, 525 (1967).
[45] H. Kanada, T. Kaneko, S. Nagata, and M. Nomoto, Prog. Theor. Phys. **61**, 1327 (1979).
[46] P. D. Miller and G. C. Phillips, Phys. Rev. **112**, 2048 (1958).
[47] T. A. Tombrello and P. D. Parker, Phys. Rev. **130**, 1112 (1963).
[48] A. C. L. Barnard, C. M. Jones, and G. C. Phillips, Nucl. Phys. **50**, 629 (1964).
[49] R. J. Spiger and T. A. Tombrello, Phys. Rev. **163**, 964 (1967).
[50] M. Ivanovich, P. G. Young, and G. G. Ohlsen, Nucl. Phys. A **110**, 441 (1968).
[51] W. R. Boykin, S. D. Baker, and D. M. Hardy, Nucl. Phys. A **195**, 241 (1972).
[52] D. M. Hardy, R. J. Spiger, S. D. Baker, Y. S. Chen, and T. A. Tombrello, Nucl. Phys. A **195**, 250 (1972).
[53] D. R. Tilley, C. M. Cheves, J. L. Godwin, G. M. Hale, H. M. Hofmann, J. H. Kelley, C. G. Sheu, and H. R. Weller, Nucl. Phys. A **708**, 3 (2002).
[54] P. D. Parker and R. W. Kavanagh, Phys. Rev. **131**, 2578 (1963).
[55] K. Nagatani, M. R. Dwarakanath, and D. Ashery, Nucl. Phys. A **128**, 325 (1969).
[56] H. Kräwinkel, H. W. Becker, L. Buchmann *et al.*, Z. Phys. A **304**, 307 (1982).
[57] J. L. Osborne, C. A. Barnes, R. W. Kavanagh, R. M. Kremer, G. J. Mathews, J. L. Zyskind, P. D. Parker, and A. J. Howard, Phys. Rev. Lett. **48**, 1664 (1982); Nucl. Phys. A **419**, 115 (1984).
[58] T. K. Alexander, G. C. Ball, W. N. Lennard, H. Geissel, and H.-B. Mak, Nucl. Phys. A **427**, 526 (1984).
[59] F. Confortola, D. Bemmerer, H. Costantini *et al.*, Phys. Rev. C **75**, 065803 (2007).
[60] T. A. D. Brown, C. Bordeanu, K. A. Snover, D. W. Storm, D. Melconian, A. L. Sallaska, S. K. L. Sjue, and S. Triambak, Phys. Rev. C **76**, 055801 (2007).
[61] A. Kontos, E. Uberseder, R. deBoer, J. Görres, C. Akers, A. Best, M. Couder, and M. Wiescher, Phys. Rev. C **87**, 065804 (2013).
[62] H. D. Holmgren and R. L. Johnston, Phys. Rev. **113**, 1556 (1959).

[63] R. G. H. Robertson, P. Dyer, T. J. Bowles, R. E. Brown, N. Jarmie, C. J. Maggiore, and S. M. Austin, Phys. Rev. C **27**, 11 (1983).
[64] M. Hilgemeier, H. W. Becker, C. Rolfs, H. P. Trautvetter, and J. W. Hammer, Z. Phys. A **329**, 243 (1988).
[65] B. S. Nara Singh, M. Hass, Y. Nir-El, and G. Haquin, Phys. Rev. Lett. **93**, 262503 (2004).
[66] D. Bemmerer, F. Confortola, H. Costantini *et al.*, Phys. Rev. Lett. **97**, 122502 (2006).
[67] Gy. Gyürky, F. Confortola, H. Costantini *et al.*, Phys. Rev. C **75**, 035805 (2007).
[68] H. Costantini, D. Bemmerer, F. Confortola *et al.*, Nucl. Phys. A **814**, 144 (2008).
[69] C. Bordeanu, Gy. Gyürky, Z. Halász, T. Szücs, G. G. Kiss, Z. Elekes, J. Farkas, Zs. Fülöp, and E. Somorjai, Nucl. Phys. A **908**, 1 (2013).
[70] M. Carmona-Gallardo, B. S. Nara Singh, M. J. G. Borge *et al.*, Phys. Rev. C **86**, 032801(R) (2012).
[71] M. Carmona-Gallardo, A. Rojas, M. J. G. Borge, B. Davids, B. R. Fulton, M. Hass, B. S. Nara Singh, C. Ruiz, and O. Tengblad, Eur. Phys. J. Web Conf. **66**, 07003 (2014).
[72] K. M. Nollett, Phys. Rev. C **63**, 054002 (2001).
[73] G. M. Griffiths, R. A. Morrow, P. J. Riley, and J. B. Warren, Can. J. Phys. **39**, 1397 (1961).
[74] S. Burzyński, K. Czerski, A. Marcinkowski, and P. Zupranski, Nucl. Phys. A **473**, 179 (1987).
[75] U. Schröder, A. Redder, C. Rolfs, R. E. Azuma, L. Buchmann, C. Campbell, J. D. King, and T. R. Donoghue, Phys. Lett. B **192**, 55 (1987).
[76] H. Utsunomiya, Y.-W. Lui, D. R. Haenni *et al.*, Phys. Rev. Lett. **65**, 847 (1990); **69**, 863 (1992).
[77] C. R. Brune, R. W. Kavanagh, and C. Rolfs, Phys. Rev. C **50**, 2205 (1994).
[78] Y. Tokimoto, H. Utsunomiya, T. Yamagata, M. Ohta, Y.-W. Lui, R. P. Schmitt, S. Typel, Y. Aoki, K. Ieki, and K. Katori, Phys. Rev. C **63**, 035801 (2001).
[79] L. R. Suelzle, M. R. Yearian, and H. Crannell, Phys. Rev. **162**, 992 (1967).
[80] G. J. C. Van Niftrik, L. Lapikás, H. De Vries, and G. Box, Nucl. Phys. A **174**, 173 (1971).
[81] F. A. Bumiller, F. R. Buskirk, J. N. Dyer, and W. A. Monson, Phys. Rev. C **5**, 391 (1972).
[82] E. F. Gibson, J. J. Kraushaar, T. G. Masterson, R. J. Peterson, R. S. Raymond, R. A. Ristinen, R. L. Boudrie, and N. S. P. King, Nucl. Phys. A **377**, 389 (1982).
[83] I. Tanihata, H. Hamagaki, O. Hashimoto, Y. Shida, N. Yoshikawa, K. Sugimoto, O. Yamakawa, T. Kobayashi, and N. Takahashi, Phys. Rev. Lett. **55**, 2676 (1985).
[84] I. Tanihata, T. Kobayashi, O. Yamakawa, S. Shimoura, K. Ekuni, K. Sugimoto, N. Takahashi, T. Shimoda, and H. Sato, Phys. Lett. B **206**, 592 (1988).
[85] H. Kanada, Q. K. K. Liu, and Y. C. Tang, Phys. Rev. C **22**, 813 (1980).
[86] T. Kajino, T. Matsuse, and A. Arima, Nucl. Phys. A **413**, 323 (1984).
[87] T. Kajino, T. Matsuse, and A. Arima, Nucl. Phys. A **414**, 185 (1984).
[88] H. Walliser and T. Fliessbach, Phys. Rev. C **31**, 2242 (1985).
[89] B. Buck, R. A. Baldock, and J. A. Rubio, J. Phys. G **11**, L11 (1985).
[90] T. Mertelmeier and H. M. Hofmann, Nucl. Phys. A **459**, 387 (1986).
[91] B. Buck and A. C. Merchant, J. Phys. G **14**, L211 (1988).
[92] T. Neff, Phys. Rev. Lett. **106**, 042502 (2011).
[93] A. Csótó and K. Langanke, Few-Body Syst. **29**, 121 (2000).
[94] S. L. Kahalas and R. K. Nesbet, J. Chem. Phys. **39**, 529 (1963).
[95] L. Wharton, L. P. Gold, and W. Klemperer, J. Chem. Phys. **37**, 2149 (1962).
[96] L. Wharton, L. P. Gold, and W. Klemperer, Phys. Rev. **133**, B270 (1964).
[97] J. C. Browne and F. A. Matsen, Phys. Rev. **135**, A1227 (1964).
[98] P. E. Cade and W. M. Huo, J. Chem. Phys. **47**, 614 (1967).
[99] S. Green, Phys. Rev. A **4**, 251 (1971).
[100] H.-G. Voelk and D. Fick, Nucl. Phys. A **530**, 475 (1991).
[101] C. F. Bender and E. R. Davidson, Phys. Rev. **183**, 23 (1969).
[102] C.-C. Lu and R. D. Present, Phys. Rev. B **1**, 2025 (1970).
[103] H. Orth, H. Ackermann, and E. W. Otten, Z. Phys. A **273**, 221 (1975).
[104] R. K. Nesbet, Phys. Rev. A **2**, 661 (1970).
[105] S. Hameed and H. M. Foley, Phys. Rev. A **6**, 1399 (1972).
[106] S. Garpman, I. Lindgren, J. Lindgren, and J. Morrison, Phys. Rev. A **11**, 758 (1975).
[107] W. Nagourney, W. Happer, and A. Lurio, Phys. Rev. A **17**, 1394 (1978).
[108] D. Sundholm, P. Pyykkö, L. Laaksonen, and A. J. Sadlej, Chem. Phys. Lett. **112**, 1 (1984).
[109] E. Rothstein, J. Chem. Phys. **50**, 1899 (1969).
[110] G. H. F. Diercksen, A. J. Sadlej, D. Sundholm, and P. Pyykkö, Chem. Phys. Lett. **143**, 163 (1988).
[111] A. J. Hebert and C. D. Hollowell, J. Chem. Phys. **65**, 4327 (1976); F. J. Lovas and E. Tiemann, J. Phys. Chem. Ref. Data **3**, 609 (1974).
[112] A. Bamberger, G. Jansen, B. Povh, D. Schwalm, and U. Smilansky, Nucl. Phys. A **194**, 193 (1972).
[113] P. Egelhof, W. Dreves, K.-H. Möbius, E. Steffens, G. Tungate, P. Zupranski, D. Fick, R. Böttger, and F. Roesel, Phys. Rev. Lett. **44**, 1380 (1980).
[114] W. J. Vermeer, M. T. Esat, M. P. Fewell, R. H. Spear, A. M. Baxter, and S. M. Burnett, Phys. Lett. B **138**, 365 (1984); W. J. Vermeer, A. M. Baxter, S. M. Burnett, M. T. Esat, M. P. Fewell, and R. H. Spear, Austral. J. Phys. **37**, 273 (1984).
[115] A. Weller, P. Egelhof, R. Čaplar *et al.*, Phys. Rev. Lett. **55**, 480 (1985).
[116] F. C. Barker, Y. Kondo, and R. H. Spear, Austral. J. Phys. **42**, 597 (1989).
[117] G. Grawert and J. Chr. Derner, Nucl. Phys. A **496**, 165 (1989).
[118] M. Bouten and M. C. Bouten, Prog. Part. Nucl. Phys. **5**, 55 (1981).
[119] O. Lutz, Phys. Lett. A **25**, 440 (1967).
[120] P. Raghavan, At. Data Nucl. Data Tables **42**, 189 (1989).
[121] A. Beckmann, K. D. Böklen, and D. Elke, Z. Phys. **270**, 173 (1974).
[122] H. Walliser, Q. K. K. Liu, H. Kanada, and Y. C. Tang, Phys. Rev. C **28**, 57 (1983).
[123] P. H. Stelson and F. K. McGowan, Nucl. Phys. **16**, 92 (1960).
[124] R. C. Ritter, P. H. Stelson, F. K. McGowan, and R. L. Robinson, Phys. Rev. **128**, 2320 (1962).

[125] O. Häusser, A. B. McDonald, T. K. Alexander, A. J. Ferguson, and R. E. Warner, Nucl. Phys. A **212**, 613 (1973); Phys. Lett. B **38**, 75 (1972).
[126] T. Kajino, G. F. Bertsch, and K.-I. Kubo, Phys. Rev. C **37**, 512 (1988).
[127] W. J. Vermeer, R. H. Spear, and F. C. Barker, Nucl. Phys. A **500**, 212 (1989).
[128] W. Nörtershäuser, D. Tiedemann, M. Žáková *et al.*, Phys. Rev. Lett. **102**, 062503 (2009).
[129] S. Kappertz, W. Geithner, G. Katko *et al.*, AIP Conf. Proc. **455**, 110 (1998).
[130] F. Ajzenberg-Selove, Nucl. Phys. A **320**, 1 (1979).
[131] S. Yu. Igashov, Comput. Math. and Math. Phys. **43**, 78 (2003).
[132] S. Yu. Igashov, in *The J-Matrix Method. Developments and Applications*, edited by A. D. Alhaidari, E. J. Heller, H. A. Yamani, and M. S. Abdelmonem (Springer, Berlin, 2008), p. 49.